Research Report

Development of calcium oxide-based sorbent for pre-combustion process

การพัฒนาตัวดูดซับแคลเซียมออกไซด์เพื่อใช้ดูดซับก๊าซคาร์บอนไดออกไซด์สำหรับกระบวนการก่อนการเผาไหม้

ชื่อผู้วิจัย

Assistant Professor Dr.Worapon Kiatkittipong / ผู้ช่วยศาสตราจารย์ ดร. วรพล เกียรติกิตติพงษ์

Dr.Suwimol Wongsakulphasatch / อาจารย์ ดร. สุวิมล วงศ์สกุลเภสัช

This research is financially supported by

Silpakorn University Research and Development Institute

(Fiscal Year 2015)

Year of completion : 2016

Acknowledgements

The authors would like to acknowledge National Research Universities and Silpakorn University Research and Development Institute, Silpakorn University for financial support.

The authors are grateful to Professor Suttichai Assabumrungrat for his valuable discussion.

Abstract

CaO-based sorbent is improved to use as adsorbent for high-temperature CO_2 sorption. In this work, CaO is derived from calcination of $CaCO_3$, which is produced by the precipitation using different precursors of calcium and carbonate. The effect of precursor (both calcium and carbonate precursors), the addition of additive, and synthesis method on CO_2 sorption capacity are subjects of investigation. The results show that the precursor has an effect on morphology of CaO derived from $CaCO_3$ and also influence on CO_2 capture ability. The CaO, which synthesized by calcium acetate with urea, show large network of connected particles, this sorbent exhibits good performance of CO_2 sorption capacity of 0.64 gCO_2/gCaO at 700oC. In addition, the addition of additive during synthesis also show the effect on CaO properties and the ability to adsorb CO_2. The sorbent prepared by adding 2 mM of Gemini surfactant provides rod-like structure with rough surface and large surface area (16.3 m^2/g). This sorbent offers CO_2 sorption capacity of 0.29 gCO_2/gCaO at 600°C. Moreover, thermal stability of CaO was improved incorporating CaO with aluminum using different techniques. The results show sorbent synthesized by sol-gel without surfactant provides good performance of CO_2 capture at 0.65 gCO_2/gCaO and stability of the sorbent show capacity reduction 35% for 10 cycles.

บทคัดย่อ

ตัวดูดซับแคลเซียมออกไซด์ได้ถูกพัฒนาเพื่อใช้เป็นตัวดูดซับแก๊สคาร์บอนไดออกไซด์ที่อุณหภูมิสูง ในงานวิจัยนี้แคลเซียมออกไซด์ได้มาจากการเผาแคลเซียมคาร์บอเนตที่สังเคราะห์ขึ้นโดยผู้วิจัยได้ศึกษาผลของสารตั้งต้น (ทั้งแคลเซียมและคาร์บอเนต) ผลของการเติมสารเติมแต่ง และผลของวิธีที่ใช้ในการสังเคราะห์แคลเซียมคาร์บอเนต ต่อคุณสมบัติในการดูดซับแก๊สคาร์บอนไดออกไซด์ ผลจากการทดลองพบว่า สารตั้งต้นที่ใช้ในการสังเคราะห์แคลเซียมคาร์บอเนตมีผลต่อคุณสมบัติของแคลเซียมออกไซด์และความสามารถในการดูดซับแก๊สคาร์บอนไดออกไซด์ แคลเซียมออกไซด์ที่ได้จากแคลเซียมคาร์บอเนตที่สังเคราะห์มาจากแคลเซียมอะซิเตตและยูเรียให้ความจุการดูดซับสูงที่สุดคือ 0.64 กรัมแก๊สคาร์บอนไดออกไซด์ต่อกรัมตัวดูดซับ ที่อุณหภูมิ 700°C ทั้งนี้เนื่องมาจากว่าอนุภาคของแคลเซียมออกไซด์ที่ได้มีขนาดเล็กและรวมตัวกันอย่างหลวมๆ นอกจากนี้ การเติมสารปรับปรุงรูปร่างด้วยสารลดแรงตึงผิวยังมีผลต่อคุณสมบัติของแคลเซียมออกไซด์และความสามารถในการดูดซับแก๊สคาร์บอนไดออกไซด์ด้วย ตัวดูดซับที่สังเคาะห์ด้วยการเติมสารลดแรงตึงผิวชนิดคู่ที่มีประจุลบหมู่ซัลเฟต ที่ความเข้มข้น 2 มิลลิโมลาร์ มีลักษณะอนุภาคคล้ายทรงกระบอกพื้นผิวขรุขระและมีพื้นที่ผิวสูงประมาณ 16.3 ตารางเมตรต่อกรัม แต่ตัวดูดซับชนิดนี้มีความสามารถในการดูดซับที่น้อยเมื่อเทียบกับตัวดูดซับชนิดที่ไม่เติมสารลดแรงตึงผิว คือ 0.29 กรัมคาร์บอนไดออกไซด์ต่อหนึ่งกรัมตัวดูดซับที่อุณหภูมิ 600 องศาเซลเซียส การทดสอบความสามารถในการทนความร้อนของตัวดูดซับได้ทำการทดสอบโดยการเติมโลหะอะลูมินาเพื่อป้องกันไม่ให้อนุภาคแคลเซียมออกไซด์เกิดการรวมตัวกันซึ่งในงานวิจัยนี้ได้ศึกษาวิธีการเตรียมตัวดูดซับว่ามีผลต่อการคงตัวของตัวดูดซับอย่างไร จากผลการทดลองพบว่าวิธีการเตรียมตัวดูดซับแบบโซลเจลให้ประสิทธิภาพในการดูดซับมากที่สุดคือ 0.65 กรัมคาร์บอนไดออกไซด์ต่อหนึ่งกรัมตัวดูดซับและพบว่าตัวดูดซับสามารถนำกลับมาใช้ใหม่ได้ 10 รอบโดยค่าความจุมีค่าลดลง 35 เปอร์เซนต์

Table of contents

List of Tables

List of Figures

1. Introduction

Hydrogen has become increasingly of great interest to use as alternative energy source for electrical power generation and as transportation fuel (Steel, 2000; Li and Cai, 2007; Kim et al., 2013). Several techniques have been developed for the production of hydrogen such as electrolysis of water, steam reforming, or partial oxidation, etc (Xiu et al., 2002). Among these, steam reforming (SR) is a conventional process that is applied for large-scale operation due to its high efficiency and low cost. However, disadvantages of this technique are still found, for example, it involves multiple steps of a typical endothermic reformer, a water-gas shift reactor and product purifications (Hufton et al., 1999). Moreover, this process has to confront with severe operating conditions in the primary reformer to obtain high conversion, thus a large amount of supplemental energy is required and expensive alloy reformer tubes must be used to withstand these harsh conditions (Lee et al., 2008). It is noted that such severe operating conditions not only make an effect to the reformer but also cause catalyst deactivation due to carbon deposition, resulting in the blockage of reformer tubes and an increase of pressure drops. According to the disadvantages mentioned above, a new developed process for hydrogen production, called sorption-enhanced steam reforming (SESR), is emerged. The concept of SESR is based on Le Chatelier's principle, of which the conversion of reactants to products and the rate of forward reaction in equilibrium can be increased by selectively removing some of the reaction products (Li and Cai, 2007; Cobden et al., 2009). By introducing an adsorbent into the reaction system for selective separation of carbon dioxide, high hydrogen purity can be obtained in a single step as steam reforming, water-gas shift, and carbon dioxide removal reactions occur simultaneously. Moreover, using sorption-enhanced steam reforming can reduce the investment cost of materials and size of vessels in commercial multiple units as well as energy consumption (Lee et al., 2008).

It has been revealed that a key to improve the overall performance of sorption-enhanced steam reforming process is the use of appropriated adsorbent material. In this work, we are therefore interested in improving sorption-enhanced steam reforming process by developing effective adsorbents for selectively removal of carbon dioxide from steam reforming reaction to enhance hydrogen production. It is reported that addressing the issue of CO_2 capture not only provide a great impact on efficient fuel utilization but also on environmental point of view. The integration of CO_2 sequestration technology with H_2 production from steam reforming as well as coal and biomass gasification could potentially result in the net removal of CO_2 from the atmosphere (Florin and Harris, 2008). Calcium oxide (CaO) is reported to be the

most suitable adsorbent for in situ CO_2 capture; however, the decay of adsorption capacity during multiple cycles is the limitation of this material. As such, our improvement is focused on increasing adsorption capacity, thermal/mechanical stability, and the ability to regenerate of CaO-based materials.

2. Objective

To improve properties of CaO-based sorbent for CO_2 capture in sorption-enhanced steam reforming reaction by focusing on the improvement of sorption capacity and thermal stability of CaO-based sorbent.

3. Literature review

Fossil and fossil derives (e.g. natural gas, methane, diesel, gasoline, methanol) and biomass derived (e.g. ethanol, glycerol, glucose) resources have been investigated to produce hydrogen-rich gas via steam reforming. Steam reforming from methane is the well-established technology at present, therefore in this work we chose steam reforming of methane to illustrate how important of sorption can enhance the reforming reaction. A brief concept of conventional steam methane reforming and sorption-enhanced steam methane reforming will be provided in this section.

Steam methane reforming

Steam reforming of methane consists of three reversible reactions: the strongly endothermic reforming reactions (1) and (2), and the moderately exothermic water-gas shift reaction (3):

$$CH_4 + H_2O \Leftrightarrow CO + 3H_2 \qquad \Delta H° = +206 \text{ kJ/mol} \qquad (1)$$

$$CH_4 + 2H_2O \Leftrightarrow CO_2 + 4H_2 \qquad \Delta H° = +165 \text{ kJ/mol} \qquad (2)$$

$$CO + H_2O \Leftrightarrow CO_2 + H_2 \qquad \Delta H° = -41 \text{ kJ/mol} \qquad (3)$$

The reforming reactions are favorable at high temperature because of the endothermic characteristic. In contrast, the exothermic shift reaction is thermodynamically favored by low temperature and unaffected by the change in pressure. The steam is normally used in excess of the stoichiometric to boost the reforming reactions and avoid carbon deposition on the catalyst, which can be occurred through direct decomposition of methane (4) or by the Boudouard reaction

(5). Note that, although using large amount of steam can enhance CH_4 conversion but additional energy to produce steam is also required.

$$CH_4\ (g) \Leftrightarrow 2H_2\ (g) + C\ (s) \qquad \Delta H° = +75\ kJ/mol \qquad (4)$$

$$2CO\ (g) \Leftrightarrow CO_2\ (g) + C\ (s) \qquad \Delta H° = -172\ kJ/mol \qquad (5)$$

In conventional steam methane reforming process, methane and steam are fed to the reformer packed with steam reforming catalyst (mostly is Ni on alumina) to form hydrogen, carbon dioxide and carbon monoxide in an endothermic reaction. These reactions are generally carried out at pressure of 14-20 atm and temperature of 800–1000°C. The products obtained from this unit are H_2, CH_4, CO, and CO_2, typically consisting of 70-72 % H_2, 6-8% CH_4, 8-10% CO, and 10-14% CO_2 on dry basis. These gases are thereafter fed to water-gas shift reactor to reduce CO content. The water-gas shift reaction can be separated into two stages: high temperature shift (HTS) and low temperature shift (LTS). The high temperature shift reactor is operated at 350-400°C and the catalyst used is Fe-Cr-based. The product stream from the first water-gas shift reactor contains 71-75 % H_2, 4-7% CH_4, 1-4% CO, and 15-20 % CO_2 on dry basis. Then, the effluent gas is sent to the low temperature shift converter, which is operated at lower temperature (200°C) with Cu-based catalyst. Water is removed from the water-gas shift product gas by condensation. In downstream, the product contains H_2 and CO_2 as the major contaminant. The contaminant CO_2 could be removed by different ways such as CO_2 amine scrubbing or pressure swing adsorption (PSA).

Steam methane reforming is a catalytic process, several catalysts have been applied for the reaction i.e. Rh, Pd, Ni, Pt, Co, etc. Among these, Nickel-based catalyst is widely used for steam methane reforming because it has high thermal stability and is more economically viable (Chanburanasiri et al., 2011). Catalysts used in the steam methane reforming reaction have to confront severe operating conditions i.e. high temperature, high pressure, and the presence of large amounts of steam. A good catalyst should be able to resist coking or decomposition by steam (Froment, 2001), inactive for side-reactions, maintains its activity at high temperature, and has high mechanical strength as well as good heat transfer properties. Although, SMR is widely applied for H_2 production; however, this process still have some limitations. Some drawbacks of the SMR process are summarized below:

- Large amount of energy is required for the reforming because it is highly endothermic reaction.

- Excess steam is needed in order to prevent carbon formation, which results in high operating cost.

- Complicated and various operating units are required in order to obtain high H_2 purity, resulting in high capital cost.

Decarbonization and CO_2 captured strategies

Generally, CO_2 is captured from the source of emissions, such as large fossil fuel or biomass energy facilities, natural gas processing, synthetic fuel plants, and fossil fuel-based hydrogen production plants. Mostly, CO_2 adsorption is involved with three different types of technologies: post-combustion, pre-combustion, and oxyfuel combustion.

- Post-combustion: The CO_2 is removed after combustion of the fossil fuel from fossil-fuel burning power plants. Here, CO_2 is captured from flue gas at power stations or other large point sources. This technology is well understood and is currently used in other industrial applications.

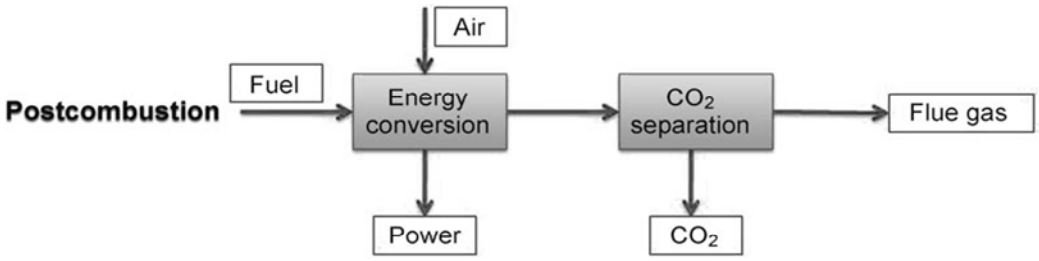

- Pre-combustion: This process separates gas CO_2 before combustion process for H_2 purification. The H_2 can then be used as fuel; the carbon dioxide is removed before combustion takes place.

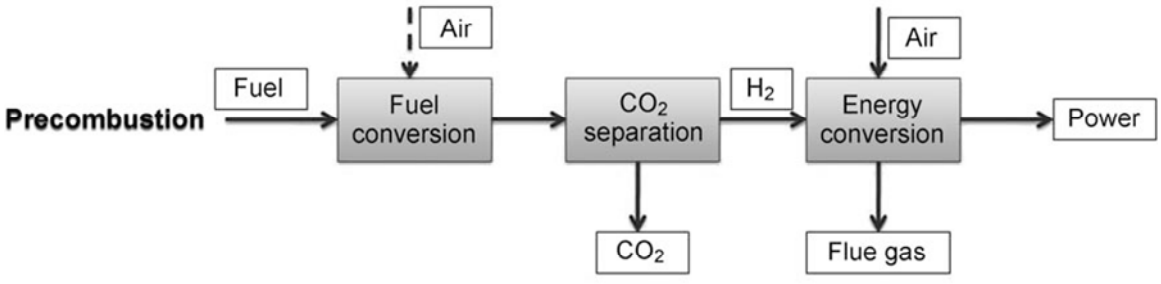

- Oxy-fuel combustion: the fuel is burned in oxygen instead of air in order to obtain rich CO_2 flue gas (ideally CO_2+H_2O), which is easy to clean and compress.

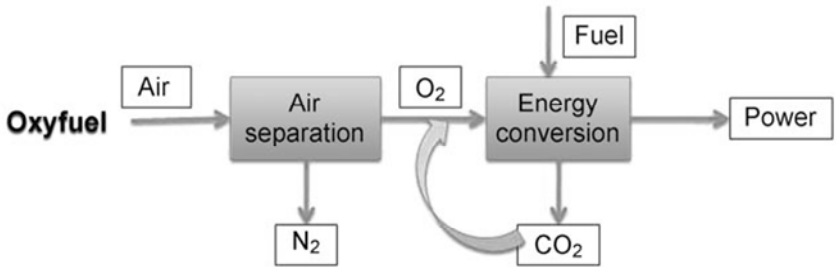

Sorption-enhanced steam methane reforming

The concept of sorption-enhanced steam methane reforming (SESMR) could be considered as an extraordinary by combining steam reforming reaction and pre-combustion for CO_2 capture. SESMR is emerged as an alternative subject to improve the conventional steam methane reforming. The concept of the SESMR is operated based on Le Chatelier's principle, of which CO_2 produced from the reforming reaction is simultaneously adsorbed by the added adsorbent, leads to the shift of reaction forward and hence an increase of the reaction rate and hydrogen yield. The SESMR system is therefore the combination of two apparatuses: reactor and adsorptive separator, which is named as adsorptive reactor. The main idea of the adsorptive reactor is the combination of reaction and adsorption by mixing catalyst and adsorbent in a single unit, resulting in a simultaneous take place of steam reforming, water-gas shift, and carbon dioxide removal reactions. CaO is widely used in SESMR process to shift equilibrium forward and then produce high hydrogen purity and yield. CaO is cheap and readily available in nature, good kinetics, high capacity and has ability to regenerate. The overall reactions occur in the adsorptive reactor unit for hydrogen production in case of using CaO as adsorbent are shown in Eqs. (6)-(9).

Reforming: $CH_4\ (g) + H_2O\ (g) \Leftrightarrow CO\ (g) + 3H_2\ (g)$ $\Delta H°=+206$ kJ/mol (6)

Water-gas shift: $CO\ (g) + H_2O\ (g) \Leftrightarrow CO_2\ (g) + H_2\ (g)$ $\Delta H°=-41$ kJ/mol (7)

CO_2 removal: $CaO\ (s) + CO_2\ (g) \Leftrightarrow CaCO_3\ (s)$ $\Delta H° = -178$ kJ/mol (8)

Overall: $CH_4\ (g) + 2H_2O\ (g) + CaO\ (s) \Leftrightarrow CaCO_3\ (s) + 4H_2\ (g)$ $\Delta H° =-13$ kJ/mol (9)

Potential advantages of SESMR can be summarized as follows:

- Simplification (or in some cases elimination) of the H_2 purification section.
- Elimination of the shift reactor(s) and shift catalysts.

• Replacement of high temperature, high alloy steels in the reforming reactor with less expensive materials of construction.

• Reduction or possible elimination of carbon deposition in the reforming reactor.

• Reduction of energy requirement.

SESMR process is typically operated in two sections in a cyclic manner. The first section is reaction-adsorption operation. The feed gas containing a mixture of CH_4 and steam is fed through a fixed bed reactor that packed with an admixture of SMR catalyst and CO_2 chemisorbent. After the reaction, the by-product CO_2 is removed from the reaction zone by the chemisorbent and a stream of H_2-rich gas is produced. At this stage, high purity of hydrogen (95+%) can be obtained. It is noted that, the adsorbent in the first section becomes gradually less efficient with operating time. As a result, the purity of main-product (H_2) correspondingly decreases and the concentration of by-product gradually increases (CO_2 and CO). There are many methods that used to regenerate of adsorbent such as pressure swing, thermal swing, purge gas stripping, displacement desorption, or reactive regeneration, etc. In general, the regeneration is not accomplished by using single step because strongly favorable interaction between CO_2 and the adsorbent. The hybrid regeneration processes are therefore necessary such as pressure swing coupled with intermediate purge. If the SESMR process is carried out by the combination of the reaction/adsorption step and the pressure swing principle, this process is called pressure swing adsorptive reactor. In the same manner, if the reaction/adsorption step combined with the temperature swing principle, it is called temperature swing adsorptive reactor.

It is known that conventional steam methane reforming is a catalytic process, choosing appropriate catalyst is therefore an essential issue for H_2 production. The catalysts in this reaction have to be operated in the severe operating conditions, high temperatures in the range of 800-1000^{o}C, pressures up to 3 MPa, and the presence of large amount of steam, depending on the feedstock. A catalyst should resist coking and the decomposition by steam, be inactive for side-reactions, maintain the activity at high temperature and have high mechanical strength as well as good heat transfer properties (Froment, 2001). The steam reforming catalyst is normally nickel (nickel supported on alumina). Note that the activities of other active metals such as cobalt, platinum, rhodium are higher than nickel but nickel is more economically viable. The catalysts that are used in the SESMR process is not significantly different from conventional steam reforming process so the high activity catalyst that is proven by steam reforming reaction can also be applied in the SEMR process. As a consequence, many researchers have been focused on an improvement of CO_2 adsorbents. Table 1 is summarized catalyst-adsorbent used for SESMR process.

Table 1: Summary of catalyst-adsorbent used for sorption-enhanced steam methane reforming process.

Catalyst	Amount (g)	Condition		CH_4 conversion (%)	H_2 concentration (%)	References
		T(°C)	S/C			
12.5wt%Ni-CaO	0.8g	600	3	86%	70%	Chanburanasiri et al. (2011)
12.5wt%Ni/Al_2O_3+CaO	0.8g+0.7g	600	3	89%	65%	
80%CaO–20%$Ca_9Al_6O_{18}$ + $Ni_{0.50}/MgAl_{2.50}$	3g+1g	600	4.2	90%	75%	Zhou et al. (2012)
CaO+ $Ni_{0.50}/MgAl_{2.50}$	2.4g+1g	600	4.2	85%	-	
16%NiO-CaO-$Ca_{12}Al_{14}O_{33}$	5g	650	3.4	70%	77%	Martavaltzi et al. (2010)
3%Ni-CaO-$Ca_{12}Al_{14}O_{33}$	12g	630	3	630°C	75%	Kim et al. (2013)
7%Ni-CaO-$Ca_{12}Al_{14}O_{33}$	12g	630	3	630°C	95%	
CaO-$Ca_{12}Al_{14}O_{33}$+Ni commercial catalyst	9g+3g	630	3	630°C	75%	
NiO-CaO	N/A	580	2	97%	98%	Ryden and Ramos (2012)

It has been proposed that the properties of the adsorbent to use in SESMR process should:

- have high adsorption selectivity and capacity for CO_2 at high temperature or in the temperature range of reforming temperature (400-600°C) and pressure (0.1-4 MPa).
- be able to withstand the high p_{steam}/p_{CO_2} ratios at the steam reforming conditions in a SESMR reactor (>20), where p_{steam} and p_{CO_2} are the partial pressures of steam and CO_2, respectively.
- have high mechanical, thermal and chemical stability for extended periods under reforming operating conditions.
- have fast kinetics of adsorption and desorption.

Generally, the adsorbents are divided into 2 groups: physisorbents and chemisorbents. The physisorbents that have been used for separation of bulk or trace CO_2 from a gas mixture are zeolites, activated carbons, silica and alumina gels. However, these sorbents have two operational limitations for use (1) equilibrium adsorption capacity of CO_2 drastically decreases at higher temperatures (above 200°C), thus, the net cyclic CO_2 adsorption capacity of the separation processes becomes impractical and (2) these adsorbents are polar adsorbents so it favorably adsorbs H_2O rather than CO_2 because of higher permanent dipole. The presence of the dilute amounts of H_2O in the gas phase may lead to the reduction of CO_2 adsorption capacity. As a consequence, the physisorbents are generally used in the process that is operated at near ambient or moderate temperature (<100°C) and without water. Chemisorbents are then turned out to be more suitable to use in SESMR process. Examples are metal oxide such as CaO and MgO, hydrotalcites, double salt, lithium metal oxide, supported sorbents. The properties of each adsorbent category are summarized in Table 2.

It is shown by the study via thermodynamic analysis that by applying SESMR for the production of hydrogen, CH_4 conversion and H_2 production can enhance. Sircar et al. (2010) studied the effect of operating temperature on concentration of H_2 for SMR and SESMR using CaO as CO_2 acceptor. It is observed that high hydrogen yield of up to 98% can be obtained at temperature between 477 and 577°C in case of SESMR while only 60-75% H_2 can be obtained at similar condition when the thermodynamic equilibrium is governed by SMR.

Table 2: Characteristics of CO_2 adsorbent materials (Reijers et al., 2006).

Group	Representative number	Adsorption capacity	Stability	Kinetics
Metal oxides	CaO	good	poor	good
Hydrotalcites	$Mg_6Al_2(OH)_{16}[CO_3].4H_2O/K_2CO_3$	poor	good	poor
Double salts	$(K_2CO_3)(2KHCO_3)(MgCO_3)(MgO).x H_2O$	fair	unknown	fair
Li metal oxides	Li_4SiO_4	fair	fair	good
Supported sorbents	CaO on Cabot Superior micropowder	fair	good	good

The CO_2 capture reaction for CaO adsorbent is occurred by the reversible reaction between CaO and CO_2, named carbonation-calcination reactions (Cobden et al., 2009; Rout et al., 2011):

$$CaO\ (s) + CO_2\ (g) \Leftrightarrow CaCO_3\ (s) \qquad \Delta H^\circ = -178\ kJ/mol \qquad (10)$$

The forward reaction, called carbonation reaction is exothermic. It occurs in the reaction-sorption step of SESMR process, where steam methane reforming (SMR) and water-gas shift (WGS) reaction take place simultaneously typical temperature of 550-650°C. On the other hand, the backward reaction, which is called calcination reaction, is endothermic and is carried out in the regeneration step of SESMR process.

Natural Ca-based adsorbents such as limestone and dolomite are availability and low cost and widely used in SESMR process; however, the disadvantages of these adsorbents are low stability (rapid decay upon multi-cycles of adsorption) and non-uniform pore size, which might affect the prediction of reaction rate. Dou et al. (2010) studied the use of low cost CaO sorbent for CO_2 capture at high temperature. The adsorbent contains about 96 wt% CaO, <2 wt% $CaCO_3$, <1 wt% MgO, <1 wt% inorganic salts, with specific surface area ca. 6 $m^2\ g^{-1}$. It was observed that the

adsorbent has very low adsorption capacity at 400-500°C; however higher adsorption capacity was found at temperature above 500°C. Broda et al. (2012) observed that by using a mixture of a 47-wt%-Ni-hydrotalcite-catalyst and limestone in SESMR process, the production of H_2 decreased with a number of adsorption cycles. It was claimed that the reduction of H_2 production is due to a decay of CO_2 uptake, which is attributed to thermal sintering. Most of the reactions of gas-solid have been known that calcination process can lead to the formation of solid layer, reducing the void fraction of the solid and hence lower adsorption ability (Rout et al., 2011). As a consequence, synthetic Ca-based sorbents are developed as an alternative strategy to improve the ability for adsorption and adsorbent regeneration.

CaO can be obtained from calcination of $CaCO_3$, which can be produced to have a variety of structure and surface property. $CaCO_3$ can crystallize and form different structures and polymorphs, depend upon the chemical and condition used (Wei et al., 2005; Yu et al., 2005; Huang et al., 2007; Chen and Xiang, 2009; Chen et al., 2010). Wei et al. (2005) synthesized $CaCO_3$ from Na_2CO_3 and $CaCl_2$ with the addition of surfactants. Three different types of anionic surfactants: sodium dodecylsulfate (SDS), sodium dodecylsulfonate (DDS), and sodium dodecylbenzenesulfonate (SDBS) were selected to study. The results showed that morphology and crystalline phase of $CaCO_3$ could be altered when surfactants were introduced into the precipitation process. At low surfactant concentration of ca. 0.05 mM, the particles obtained from the presence of all anionic surfactants are rhombohedral calcite crystals. When surfactant concentration was increased to 0.5 mM, vaterite crystals were produced in SDBS system, while no obvious change was observed for SDS and DDS systems. As the concentration was further increased to 5 mM, vaterite particles were formed in SDBS system, and hollow-spherical calcite crystals obtained in the presence of SDS, whereas rhombohedral calcite crystals were observed in DDS system. Altay et al. (2007) investigated the use of additive, mixing and aging temperature for the synthesis of $CaCO_3$ from the solutions of $CaCl_2$ and Na_2CO_3. It was found that the presence of the additives, PDDA, CTAB, and EDTA suppressed the formation of aragonite. When PDDA of 1 g/L was added, only calcite polymorph was obtained at all temperatures. The morphology of $CaCO_3$ controlled by CTAB surfactant was calcite with rhombohedra and plate-like crystal morphology at either 30 or 50°C. At higher temperature of 70°C, calcite and aragonite particles were observed with rhombohedra shape of calcite and branch-like shape of aragonite. The rhombohedra shapes were observed at 90°C but aragonite crystal was observed more than calcite. For the case of EDTA, it was shown that EDTA has the strongest effect on $CaCO_3$ morphology. At EDTA concentration of 1 g/L, calcite

particles with apple core-type morphology were observed. With increasing temperature to 50°C, calcite structure was formed with the same apple core morphology but with less particle size variation. In addition, the study was also observed that pH of solution and concentration of surfactant are factors that can influence the formation of $CaCO_3$. Chen and Xiang (2009) studied the effect of reaction temperature on structure and morphology of $CaCO_3$ synthesized from $CaCl_2$ and NH_4HCO_3. Lamellar vaterite were formed at reaction temperature of 30-40°C while aragonite and calcite were observed at 50-70°C. At high temperature of 80°C, the aragonite whiskers were produced.

Although synthetic CaO can provide uniform pore size, particle size, and high surface adsorption area; however, the synthetic CaO has not been widely developed for CO_2 capture in the sorption-enhanced reaction process as a number of carbonation-calcination cycles is still low. Sintering of the sorbent is a cause of a reduction of calcium looping cycle. High operating temperature can induce the sorbent to aggregate, which is resulted in the changes in pore shape and a reduction of pore size CaO and hence total surface area (Blamey et al., 2010). Lee et al. (2007) reported that critical problem of using CaO as the adsorbent is an operating at high temperature of regeneration. Typically, a temperature for this purpose is 850-1000°C, this can cause the rapid decay of calcium-based adsorbents in capacity upon multiple cycles of use. To solve this problem, some techniques such as co-addition of inert support or metal oxide, thermal/water pretreatment, pelletization, etc., have been developed (Blamey et al., 2010).

Harrison et al. (2009) presented that the improvement of the durability of CaO adsorbent can be made by synthetic CaO-based sorbents which are stronger than the natural limestone and dolomites. This synthetic material can be seen in the literature of Li et al. (2006), where they claimed that CaO-based acceptor can be synthesized with a capacity of 0.45 g CO_2/g acceptor and the adsorbent do not degrade upon multi-cycle test with calcination under mild condition. This acceptor consists of CaO (75%) supported on $Ca_{12}Al_{14}O_{33}$ (25%). Similarly, Feng et al. (2006) reported that CaO supported on γ-Al_2O_3 did not lose its capacity up to nine cycles. The second approach of CaO durability improvement involves modification of CaO. It was found that the adsorbent activity could be restored through hydration forming $Ca(OH)_2$ (Manovic et al., 2012). Table 3 is summarized the improvement of CaO-based sorbenet for CO_2 capture.

Table 3: Summarization of the improvement of CaO-based sorbent for CO_2 capture.

CaO-based sorbents	Surface area (m^2/g)	Pore volume (cm^3/g)	Number of cycles	Maximum capacity	References
$CaO/Ca_{12}Al_{14}O_{33}$	18.53	N/A	50	0.52 gCO_2/ gsorbent	Cai et al. (2006)
CaO/SBA-15	155	0.432	40	0.53 gCO_2/ gsorbent	Huang et al. (2010)
CaO/Al_2O_3	N/A	N/A	30	50 gCO_2/ gsorbent	Florin and Fennell (2011)
CaO/Kaoli/ $Al(OH)_3$	36.2	0.082	30	0.13 gCO_2/ gsorbent	Ridha et al. (2012)
CaO/Titanium ethoxide	13.8	3.30	30	N/A	Vieille et al. (2012)
$CaO/Mn(NO_3)_2$, $CaO/MnCO_3$	N/A	N/A	100	0.012 gCO_2/ gsorbent	Sun et al. (2012)

4. Experimental

In this work, subjects to improve CaO properties for high-temperature CO_2 sorption were investigated in two main topics: 1) improvement of sorption capacity and 2) improvement of the stability of CaO. Details of experimental procedure for each topic are provided below.

4.1 Material preparation

4.1.1 Subject of improving adsorption capacity

4.1.1.1 Preparation of $CaCO_3$

- Investigating the effect of calcium precursors ($CaCl_2$ and $Ca(CH_3COO)_2$) and carbonate precursors (Na_2CO_3 and $CO(NH_2)_2$) on CO_2 sorption capacity. In case of Na_2CO_3 precursor, 100-mL of 2.5 M $CaCl_2$/$Ca(CH_3COO)_2$ solution was mixed with equimolar concentration of 100-mL Na_2CO_3. The mixture was stirred for 3 h at room temperature and the reaction was allowed to maintain for 5 h. The precipitate was filtered, washed with distilled water 3 times, and dried at 30°C. In case of using $CO(NH_2)_2$ as carbonate precursor, 100 mL of 2.5 M $CaCl_2$/$Ca(CH_3COO)_2$ solution was mixed with equimolar concentration of 100-mL $CO(NH_2)_2$ under vigorous stirring at 90°C for 24 h. The obtained precipitate was filtered, washed with distilled water, and dried at 30°C.

- Investigating the effect of morphology, structure, and surface area on CO_2 capture by using surfactants as structure-directing agent for the synthesis of $CaCO_3$. $CaCO_3$ was prepared by dissolving 100 mL of 2.5 M of $Ca(CH_3COO)_2$ with a desired concentration of SDS or Gemini surfactant. Then $CO(NH_2)_2$ (carbonate precursor) solution was added into the mixture solution under vigorous stirring at 90°C for 24 h. The obtained precipitate was filtered, washed with distilled water, and dried at 30°C. The concentrations of surfactant were used at, 10, 20, 40 mM of SDS, and 0.045, 0.08, 0.12, 2, and 4 mM of Gemini surfactant (12-4-12^{-}). Similarly, the products were denoted as $CaCO_3$-SDS xx mM, and $CaCO_3$-GS xx mM, where xx stands for concentration of SDS or Gemini surfactant.

4.1.1.2 Preparation of CaO

To produce CaO sorbents for CO_2 capture, $CaCO_3$ samples were calcined under air at 850°C for 30 min.

4.1.2 Subject of improving sorbent stability

In this section, CaO-based sorbents have been prepared by different methods including co-precipitation, wet mixing, sol-gel, and sol mixing. Each method is summarized as follows:

- Co-precipitation method

For co-precipitation method, CaO-based sorbent was prepared by mixing the solution of $Ca(CH_3COO)_2$ and $Al(NO_3)_3$, and then urea solution was added into the mixture. The ratio of calcium and alumina was set at 70:30 by weight, where equimolar of metal and urea of 2.5 M (100 ml) was mixed. For the sample with the addition of Gemini surfactant, 0.35 g of Gemini surfactant was added to obtain 2 mM concentration in metal solution (Calcium and Aluminum). Then the solution of urea was added into the mixture solution under vigorous stirring at 90°C for 24 h. The obtained precipitate was filtered, washed with distilled water, and dried at 30°C. The

powder was calcined at 800°C for 2 h. The products were denoted as Co-precipitation and Co-precipitation-GS 2 mM.

- Wet mixing method

$Ca(CH_3COO)_2$ (6.60 g) and $Al(NO_3)_3$ (3.76 g) were mixed in DI-water to obtain calcium to alumina ratio of 70:30%wt. The mixture solution of metal and 2 mM of Gemini surfactant was allowed to stir at 75°C for 1 h and then the solution was dried in an oven at 110°C for 12 h. The white powder was calcined at 900°C for 1.5 h. The products were denoted as Wet mixing and Wet mixing-GS 2 mM.

- Sol-gel combustion method

The sol-gel combustion was synthesized with using $Ca(NO_3)_2$ and $Al(NO_3)_3$ as precursors. To obtain calcium to alumina ratio of 70:30%wt, 4.22 g of calcium was mixed with 2.31 g of alumina in DI water. Then, citric acid 5.02 g was added into the solution to be an ignitor during calcination. The solution was continuously stirred at 80°C for 7 h. After that, the mixture solution was placed at ambient temperature for 18 h. The solution, which obtained as wet gel, was dried at 80°C for 5 h and 110°C for 12 h. The dried gel was quickly calcined at 850°C for 2 h and white powder was obtained. For the case of adding Gemini surfactant, 0.024 g of Gemini surfactant was added into the solution containing citric acid, $Ca(NO_3)_2$, and $Al(NO_3)_3$. The rest of the method was followed as same as those carried out without adding surfactants. The sorbents were denoted as Sol-gel and Sol-gel-GS 2 mM.

- Sol mixing method

In sol mixing technique, 2.68 g of $Al(NO_3)_3$ and 1.5 g of CaO, and 2 mM of Gemini surfactant, were dissolved in DI-water and allowed to stir at 75°C for 1 h. The mixture solution was placed at room temperature for 24 h, dried at 110°C for 24 h. The solid was calcined at 850°C for 1.5 h. The sorbents were denoted as Sol mixing.

4.2 Material characterization

Crystalline structure, morphology, and phase composition of the as-synthesized $CaCO_3$ and CaO were examined by using X-Ray diffraction (XRD) technique. Compositions of $CaCO_3$ and CaO were determined by hydration method and Thermogravimetric analysis. Surface area, pore size, and pore volume were measured by Nitrogen adsorption/desorption technique. Textural properties were examined by scanning electron microscopy (SEM).

4.3 CO_2 sorption capacity and sorbent stability tests

Evaluation of CO_2 sorption capacity and sorbent stability were conducted experimentally using fixed-bed reactor. For each experiment, the length bed of sorbent was fixed at 7.5 cm and heated from ambient temperature to 850°C under N_2 flow and held for 30 min before taking measurement in order to refresh the

material. CO_2 sorption (carbonation reaction) was carried out at 600ºC under 15 mL min^{-1} gas flow containing 15% CO_2 (balanced N_2). For desorption test (calcination reaction), the sample was heated to 850ºC under 100% N_2 for 30 min (or until no CO_2 was observed).

The stability of the sorbent was determined by examining a number of carbonation (600 ^{o}C)/calcination (850 ^{o}C) cycles that could maintain high sorption capacity. Each condition was repeated twice and the results are shown in average value.

5. Results and discussion

5.1 Effect of calcium and carbonate sources

5.1.1 Characteristic and properties of sorbents

Phase compositions of the synthesized $CaCO_3$ with different calcium precursors examined by XRD are shown in Fig. 1. The results show that calcite is observed with the sorbent synthesized from calcium chloride precursors, $CaCO_{3,Cl\text{-}Na}$ and $CaCO_{3,Cl\text{-}Urea}$. Mixed phases of calcite (30%) and vaterite (70%) is found with $CaCO_{3,Ac\text{-}Na}$ whereas aragonite is observed with $CaCO_{3,Ac\text{-}Urea}$.

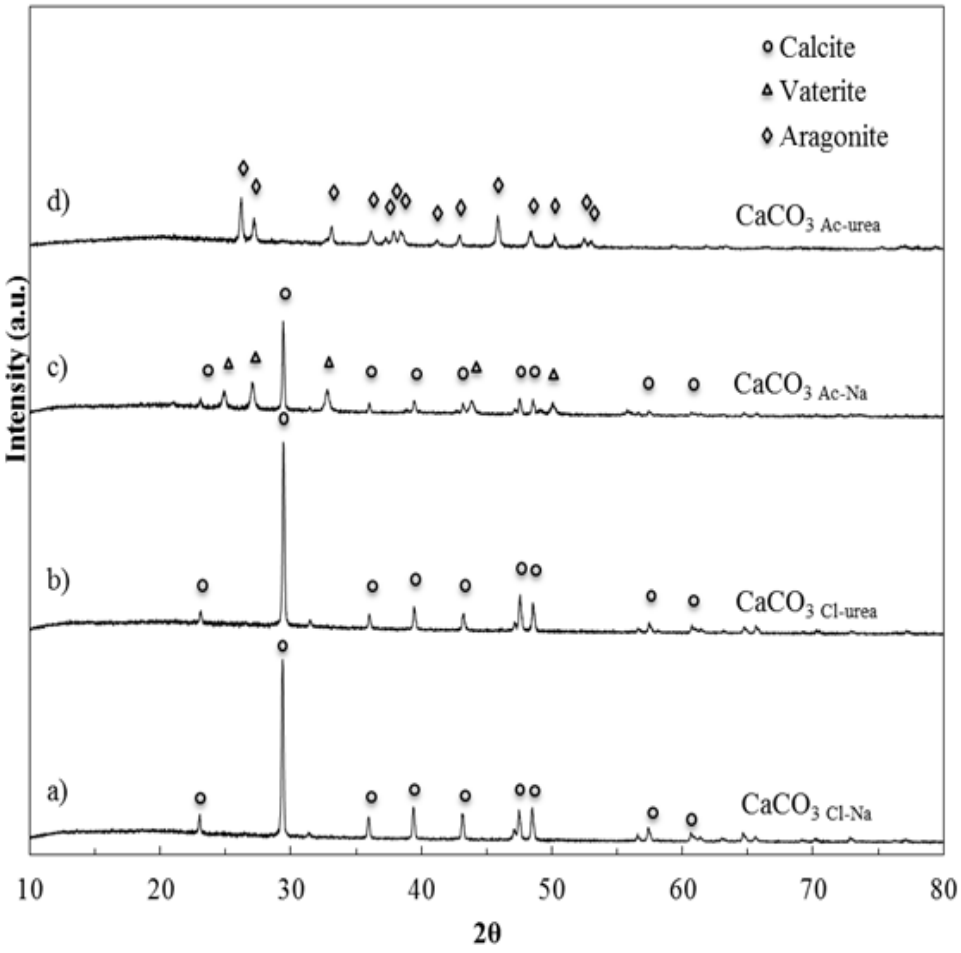

Fig. 1: XRD patterns of $CaCO_3$ synthesized from different calcium and carbonate precursors a) $CaCO_{3\ Cl\text{-}Na}$, b) $CaCO_{3\ Cl\text{-}urea}$, c) $CaCO_{3\ Ac\text{-}Na}$, and d) $CaCO_{3\ Ac\text{-}urea}$.

SEM images of $CaCO_3$ samples are presented in Fig. 2. The results of precipitation by different precursors show morphology of the samples differ significantly; $CaCO_{3,Cl\text{-}Na}$ exhibits agglomeration of small cubic (rhombohedral) particles with particle size ranging in between 0.5 and 2 μm. $CaCO_{3,Cl\text{-}Urea}$ possesses spherical particles with rough surface with an average size of approximately 1 μm, $CaCO_{3,Ac\text{-}Na}$ has spherical-like morphology with smooth surface and an average particle size of 0.5 to 2 μm. $CaCO_{3,Ac\text{-}Urea}$ shows aggregated form of $CaCO_3$ particles with large particle.

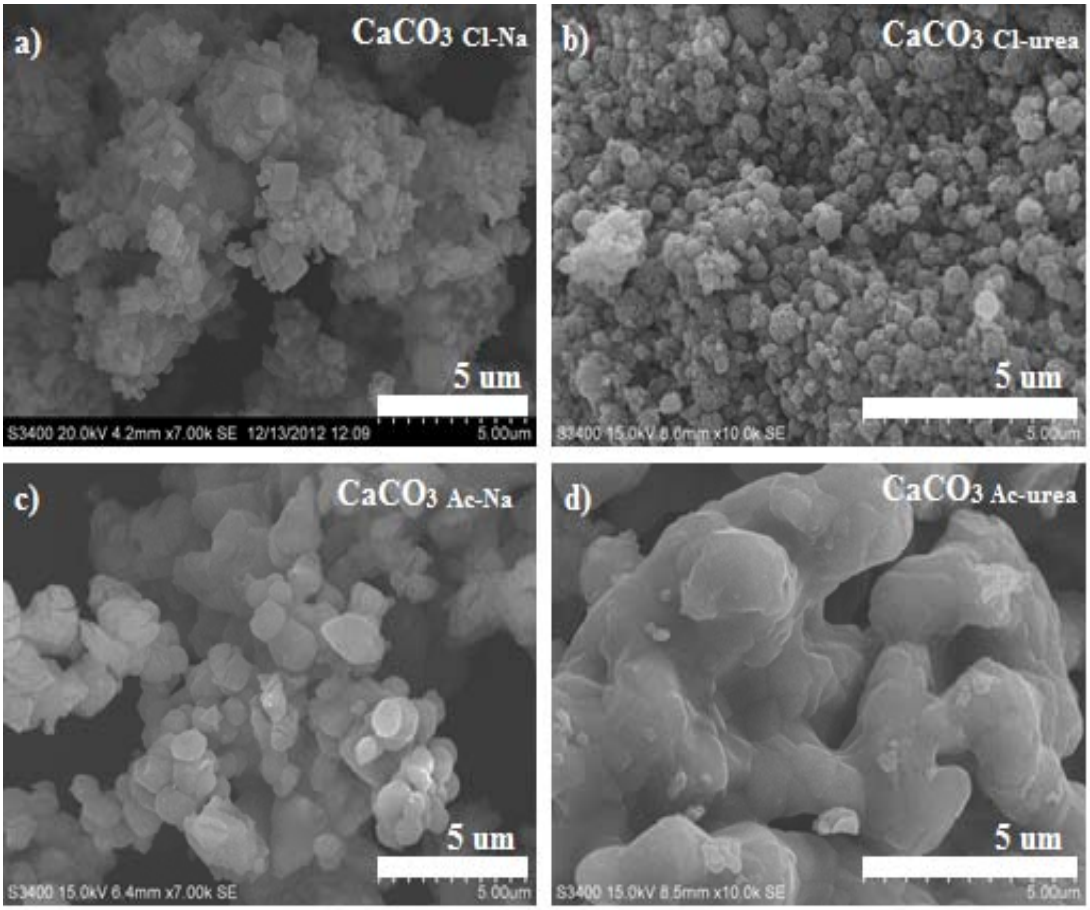

Fig. 2: SEM images of $CaCO_3$ synthesized from different calcium and carbonate precursors a) $CaCO_{3\ Cl\text{-}Na}$, b) $CaCO_{3\ Cl\text{-}urea}$, c) $CaCO_{3\ Ac\text{-}Na}$, and d) $CaCO_{3\ Ac\text{-}urea}$.

In order to obtain CaO for CO_2 sorption test, synthetic $CaCO_3$ has to be calcined to decompose into CaO. We firstly checked the temperature requirement for the complete decomposition of $CaCO_3$ into CaO by TGA analysis. The results of TGA measurements presented in Fig. 3 show that all $CaCO_3$ sorbents have approximately 44 %wt loss of CO_2 which indicates the decomposition of $CaCO_3$ to CaO when $CaCO_3$ was heated to high temperature. $CaCO_{3,Cl\text{-}Na}$ shows weight loss at 528°C, $CaCO_{3,Cl\text{-}urea}$ at 577°C, $CaCO_{3,Ac\text{-}Na}$ decomposes CO_2 at 552°C, and decomposition of $CaCO_{3,Ac\text{-}urea}$ is observed at 541°C. For all samples, complete weight loss of $CaCO_3$ to CaO is shown in the temperature range of 700-800°C so it could be concluded here that in order to ensure that pure CaO could be obtained, the $CaCO_3$ sample should be calcined at temperature higher than 850°C. Note that the decomposition of $CaCO_3$ to CaO exhibits endothermic reaction.

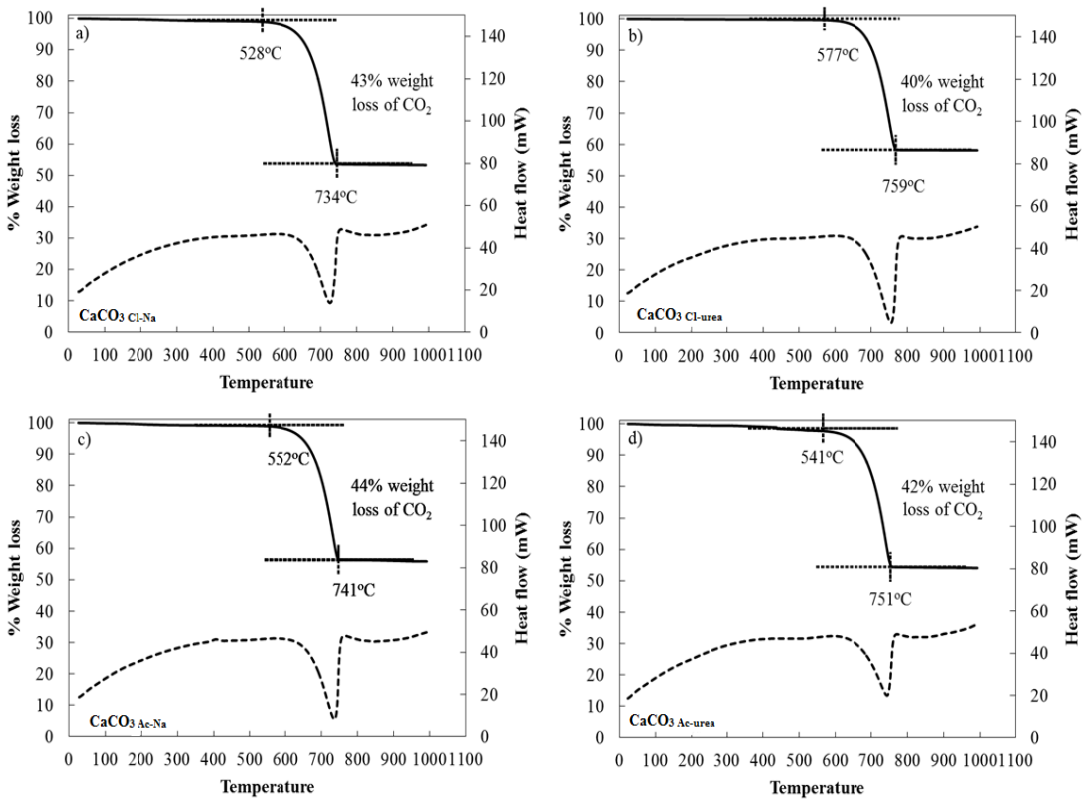

Fig. 3: TGA results of weight decomposition a) $CaCO_{3,Cl\text{-}Na}$, b) $CaCO_{3,Cl\text{-}urea}$, c) $CaCO_{3,Ac\text{-}Na}$, d) $CaCO_{3,Ac\text{-}urea}$.

XRD pattern of CaO sorbents derived from different $CaCO_3$ precursors are shown in Fig. 4. All samples exhibit major peaks at 2θ of 32.2, 37.4, 53.9, 64.2, and 67.4, corresponding to CaO phase (Akgsornpeak et al., 2014; Cho et al.,2009; Lu et al., 2008). This result indicates complete decomposition of $CaCO_3$ can be obtained at 850°C regardless of $CaCO_3$ precursors, which is in agreement with TGA results demonstrated in Fig. 3.

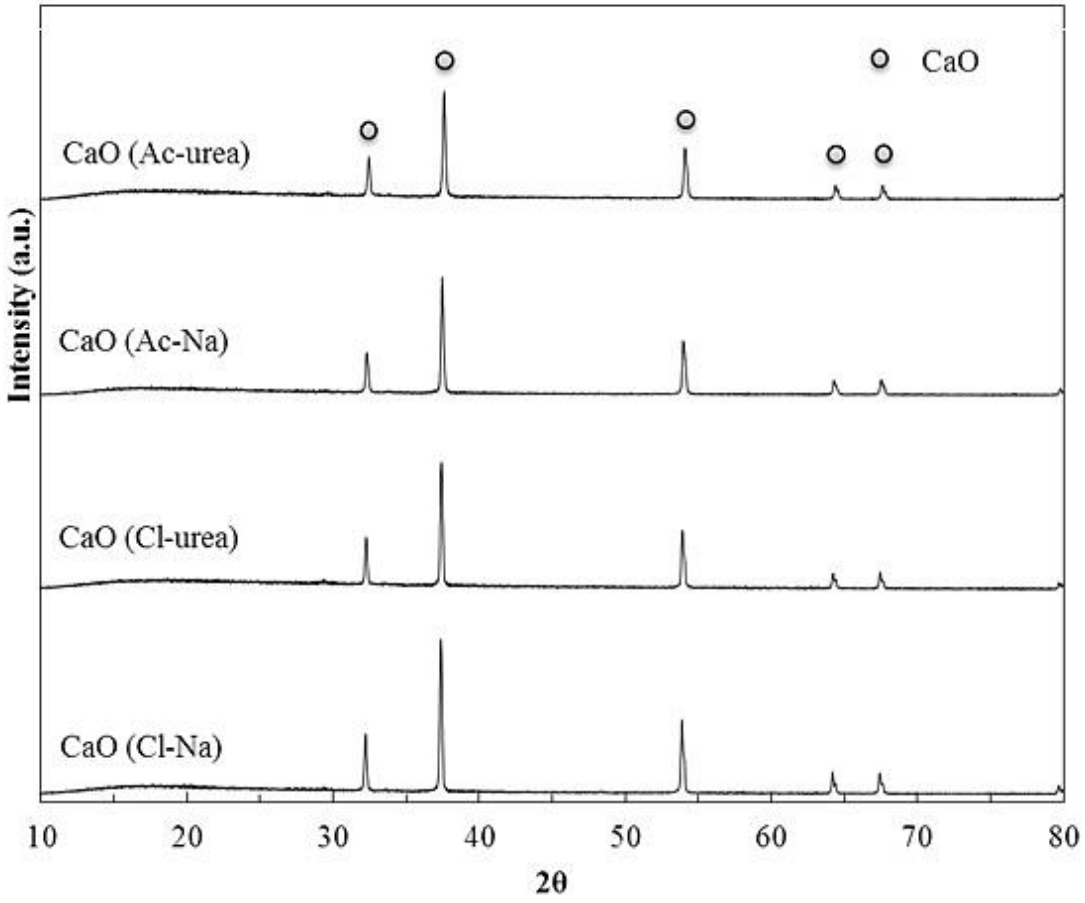

Fig. 4: XRD patterns of CaO derived from different calcium carbonate precursors a) $CaO_{Cl\text{-}Na}$, b) $CaO_{Cl\text{-}urea}$, c) $CaO_{Ac\text{-}Na}$, d) $CaO_{Ac\text{-}urea}$.

SEM images of CaO samples are depicted in Fig. 5. The results of all CaO sorbents obtained from precipitation of $CaCO_3$ show aggregated particles after calcination. $CaO_{Cl\text{-}Na}$ exhibits agglomeration of small particles. $CaO_{Ac\text{-}Na}$ has oval-like particles with smooth surface morphology having average size of approximately 2 μm. $CaO_{Ac\text{-}urea}$ has large network of connected particles with particle size ranging from 0.5 μm to 2 μm.

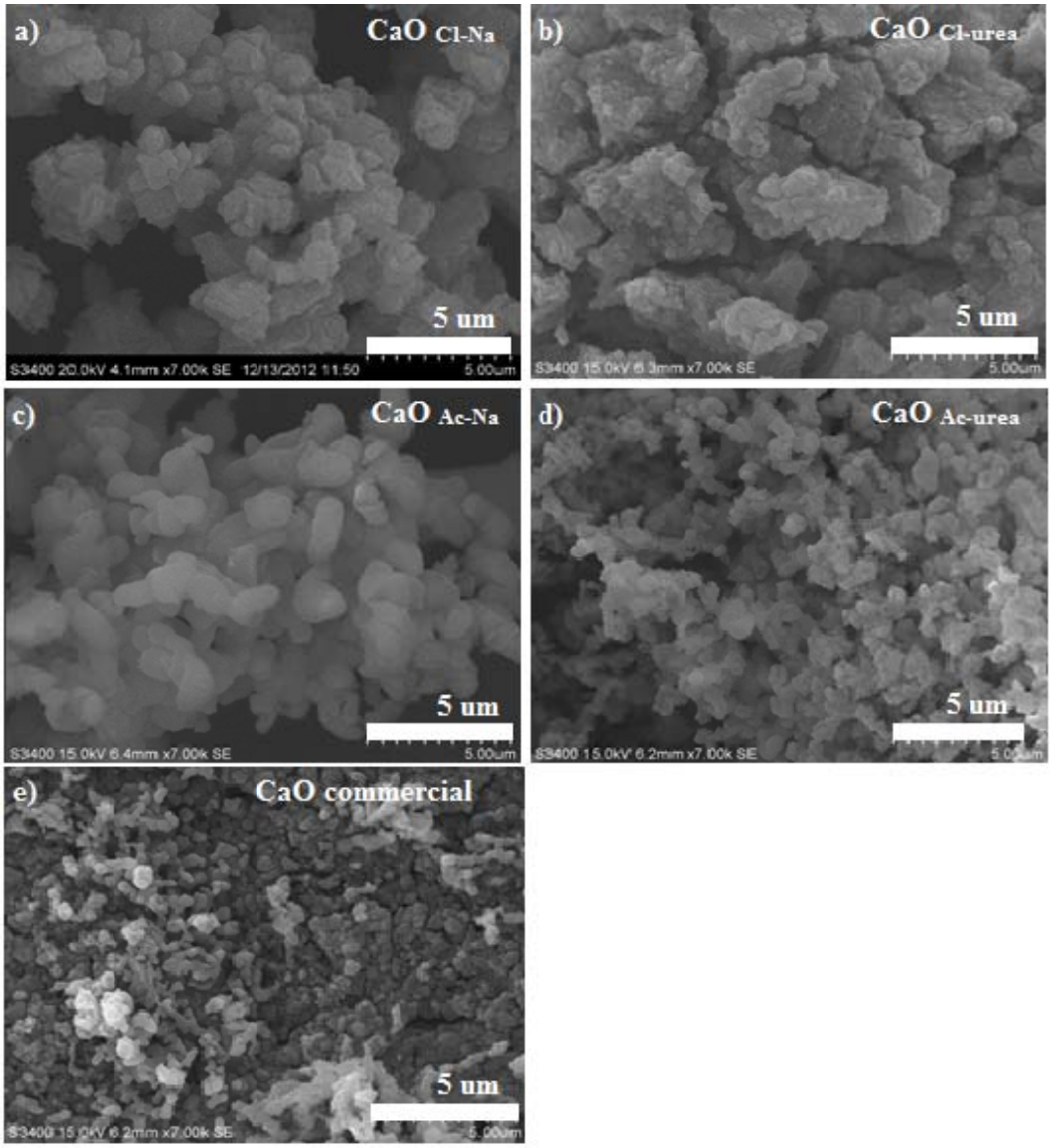

Fig. 5: SEM images of CaO synthesized from different calcium and carbonate precursors a) $CaO_{Cl\text{-}Na}$, b) $CaO_{Cl\text{-}urea}$, c) $CaO_{Ac\text{-}Na}$, d) $CaO_{Ac\text{-}urea}$, e) CaO commercial.

Table 4 presents textural properties of CaO sorbents derived from different $CaCO_3$ sources. Large surface area, pore volume, and pore size diameter are observed with $CaO_{Ac\text{-}urea}$ and these values are significant deviated from other sorbents. Note that the synthetic CaO sorbents possess higher BET surface area double in magnitude than that of commercial CaO, implying that the synthetic CaO samples have higher CO_2 sorption capability. Crystallized size of CaO calculated from Scherrer equation at the highest peak of CaO of 37.4° is also shown in Table 1 and the crystallized size is in the order: $CaO_{Cl\text{-}urea} > CaO_{Cl\text{-}Na} > CaO_{Ac\text{-}Na} > CaO_{Ac\text{-}urea}$.

Table 4: Textural properties of CaO sorbents

Sample	Surface area (m^2/g)	Pore volume (cm^3/g)	Pore size diameter (nm)	Crystal size
$CaO_{Cl\text{-}Na}$	4.8	0.012	12.2	52.01
$CaO_{Cl\text{-}urea}$	8.4	0.033	14.6	54.37
$CaO_{Ac\text{-}Na}$	8.0	0.024	10.7	45.8
$CaO_{Ac\text{-}urea}$	9.8	0.063	27.5	44.27
$CaO_{Commercial}$	4.8	0.012	9.7	-

5.1.2 CO_2 sorption tests

Fig. 6 presents conversion of CaO for CO_2 capture at temperature ranging from 600-700 $^{\circ}C$. It is worth to note than the results shown in Figs. 6 (a-e) are the mean values of two experiments each performed in duplicate; error bars are not placed in the figure for clarity of data. The standard deviation less than 2.5 % in all duplicate indicated a good reproducibility. As a matter of good scientific practice, a significance level is chosen before data collection and is often set to 0.05 (5%) (Craparo, 2007). Differences in sorption performance among the sorbents are therefore statistically significant. The results in Fig. 6a show that conversion of $CaO_{Cl\text{-}Na}$ increases with increasing carbonation temperature, indicating higher sorption is preferable at elevated temperature. This might be due to an increase of sorption rate at elevated temperature, where CO_2 molecules can access to the available active CaO easier than that at low temperatures. Our results are in good agreement with those reported by Florin and Harris (2008), of which their thermodynamic data showed equilibrium partial pressure of CO_2 increased with increasing carbonation temperature: equilibrium CO_2 partial pressure at 600$^{\circ}C$, 650$^{\circ}C$ and 700$^{\circ}C$ showed 0.006, 0.01 and 0.04 atm, respectively. By comparison of CO_2 uptake capacity at the same sorption temperature, it is found that $CaO_{Ac\text{-}urea}$ offers higher sorption capacity than others. This might be due to $CaO_{Ac\text{-}urea}$ possesses high surface area and small particle, which enhances the accessibility of CO_2 molecules to adsorb on CaO. In addition, $CaO_{Cl\text{-}urea}$ also show a good performance on CO_2 capture as a fair sorption

capacity is observed when compared with the sorbents synthesized using sodium as carbonate precursors. It could be concluded here that using urea as carbonate precursor offers higher sorption capacity than using sodium as precursor.

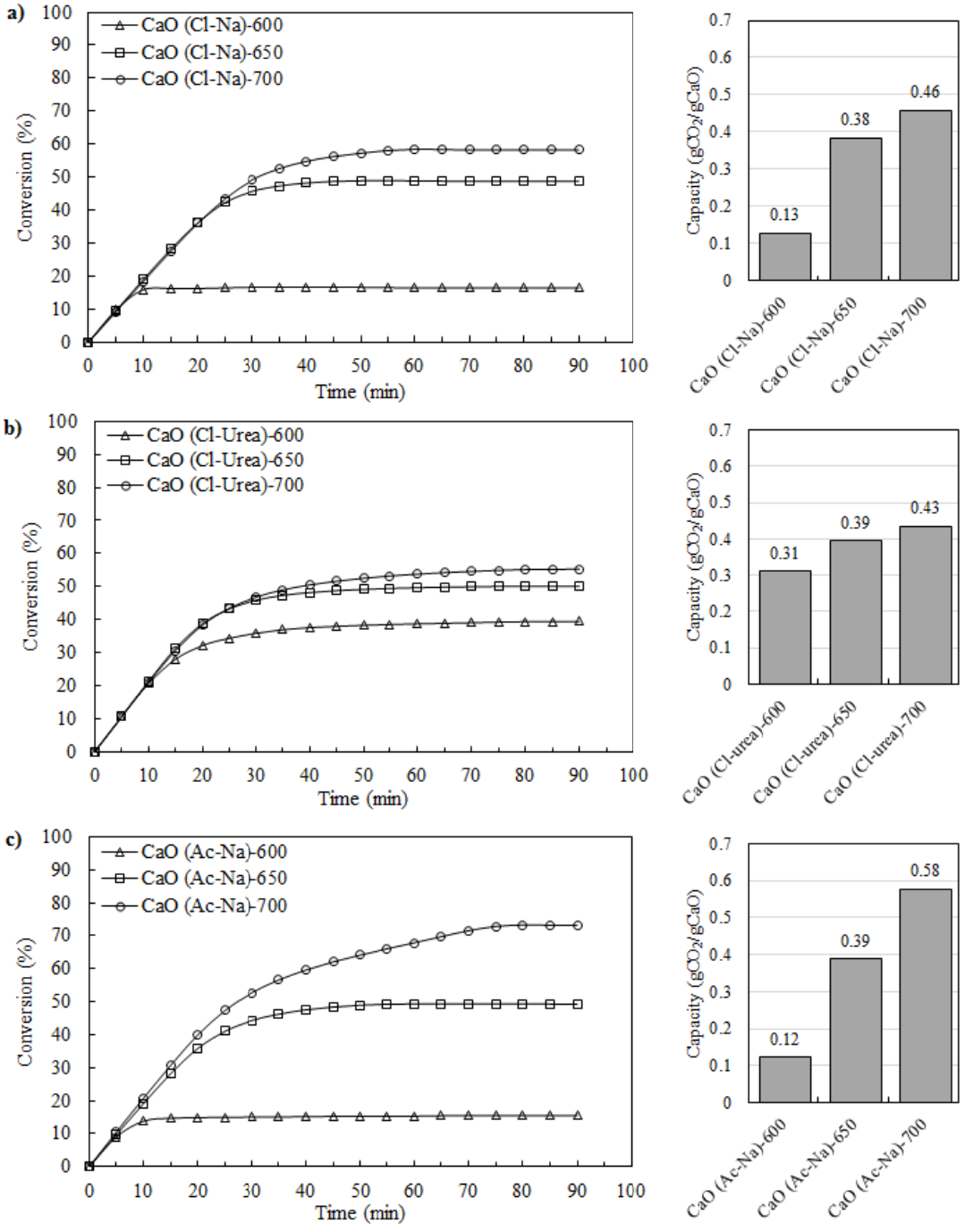

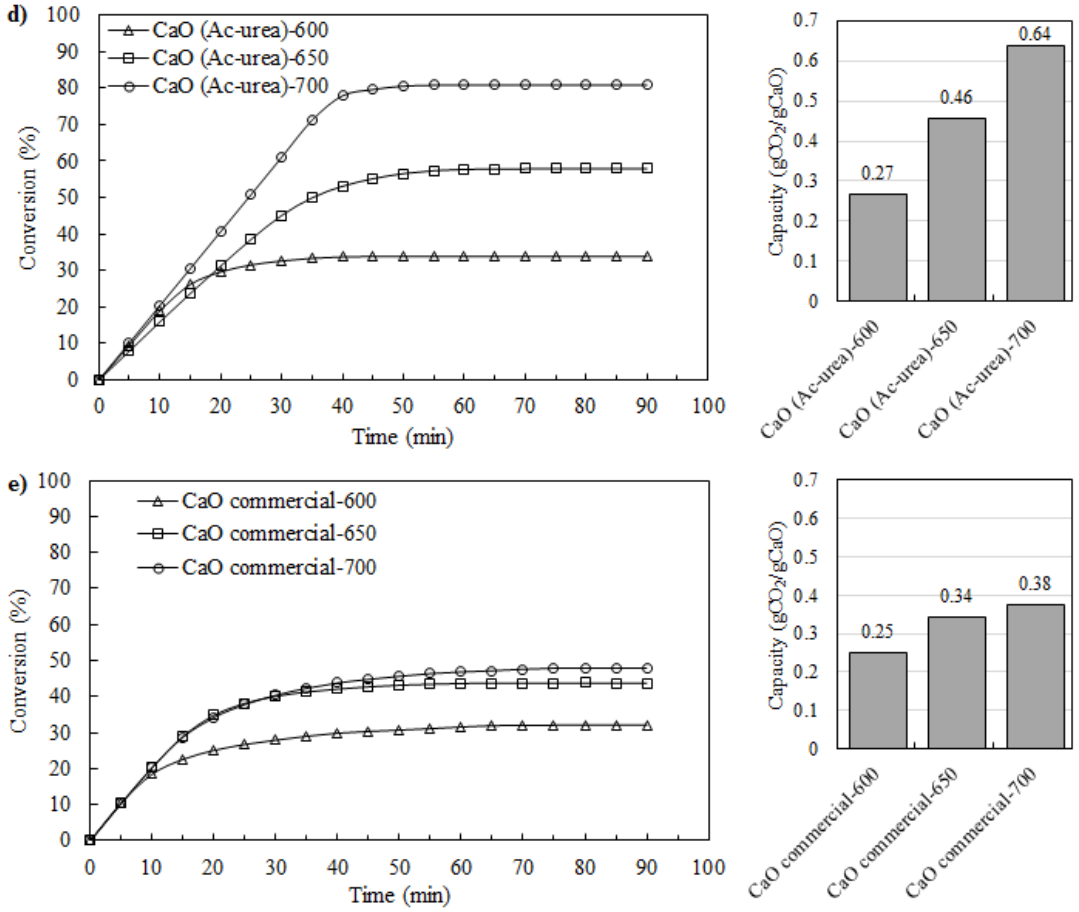

Fig. 6: Conversion of CaO synthesized from different $CaCO_3$: a) $CaO_{Cl\text{-}Na}$, b) $CaO_{Cl\text{-}urea}$, c) $CaO_{Ac\text{-}Na}$, d) $CaO_{Ac\text{-}urea}$, f) $CaO_{commercial}$.

Reaction kinetics of CO_2 and CaO particle were investigated using shrinking-core model as the reaction is likely to be governed by both chemical reaction at the surface and the product layer diffusion. The particle of CaO sorbent was assumed to be spherical grain and the sorption process was isothermal system. A model of the reaction core considers the change in radius of particle, which is given by Dou et al. (2010):

$$\frac{r^3}{r_0^3} = 1 - \alpha x, \tag{15}$$

where r_0 is the initial particle radius and r is particle radius at time t. The shrinkage factor, α, is defined as:

$$\alpha = \frac{\Delta v_i}{\Delta v_i^{t=0}}, \tag{16}$$

where i represents single volume element, Δv_i is the volumetric shrinkage rate at time t, and $\Delta v_i^{t=0}$ is the volumetric shrinkage rate at time t=0.

It was proposed that if the reaction is controlled by chemical reaction at the surface, the shrinking-core model is expressed as:

$$\frac{t_g}{\tau_g} = 1-(1-\alpha x)^{1/3} = g(x), \tag{17}$$

where t_g is the reaction time and is defined as:

$$t_g = \frac{\rho_s r_0 (1-(r/r_0))}{b k_s c_0}, \tag{18}$$

ρ_s is density of the particle, k_s is rate constant of surface chemical reaction, b is stoichiometric coefficient.

The parameter τ_g is the time required for complete conversion $(x=1)$ of the sorbent and can be calculated from

$$\tau_g = \frac{\rho_s r_0}{b k_s c_0}. \tag{19}$$

If the reaction is controlled by mass transfer diffusion through the product layer, the model is expressed as:

$$\frac{t_g}{\tau_p} = 1-3(1-\alpha x)^{2/3} + 2(1-\alpha x) = p(x), \tag{20}$$

where

$$\tau_p = \frac{\rho_s r_0^2}{6 b D_e c_0}, \tag{21}$$

D_e is the effective diffusion coefficient.

If the reaction is controlled by both surface reaction and mass transfer diffusion, the model can be rationale as:

$$\frac{t-t_b}{\tau_g} = g(x) + \delta^2 p(x), \tag{22}$$

where t_b is breakthrough time, and

$$\delta^2 = \frac{\tau_P}{\tau_g} = \frac{k_s r_0}{6 D_e}. \tag{23}$$

The parameter δ^2 is the shrinking core reaction modulus defined as the ratio of product layer diffusion resistance to surface reaction resistance. The reaction is suggested to be surface reaction control when $\delta^2 << 1$ whereas product layer diffusion control is reliably assumed when $\delta^2 > 10$. Intermediate values of δ^2 are suggested to be controlled by both surface reaction and layer diffusion.

The calculation of kinetics (Fig. 7) shows that diffusion control is observed at 600°C for all sorbents as indicated by the values of $\delta^2 > 10$. This might be due to low kinetic rate of CO_2 molecules, leading to low ability in diffusing through the layer of $CaCO_3$. When temperature was increased to 650°C and 700°C, surface reaction tend to become predominant as shown by a decrease of δ^2 value for all sorbents except for $CaO_{Cl\text{-}Na}$ and $CaO_{commercial}$. This possibly be because increasing temperature could increase acceleration of CO_2 molecules. No sorbent sample has δ^2 less than 1, indicating the sorption system is controlled by both surface and diffusion through the layer of $CaCO_3$, which is the nature of CaO sorbent as reported by Cazorla-Amorb et al. (1991).

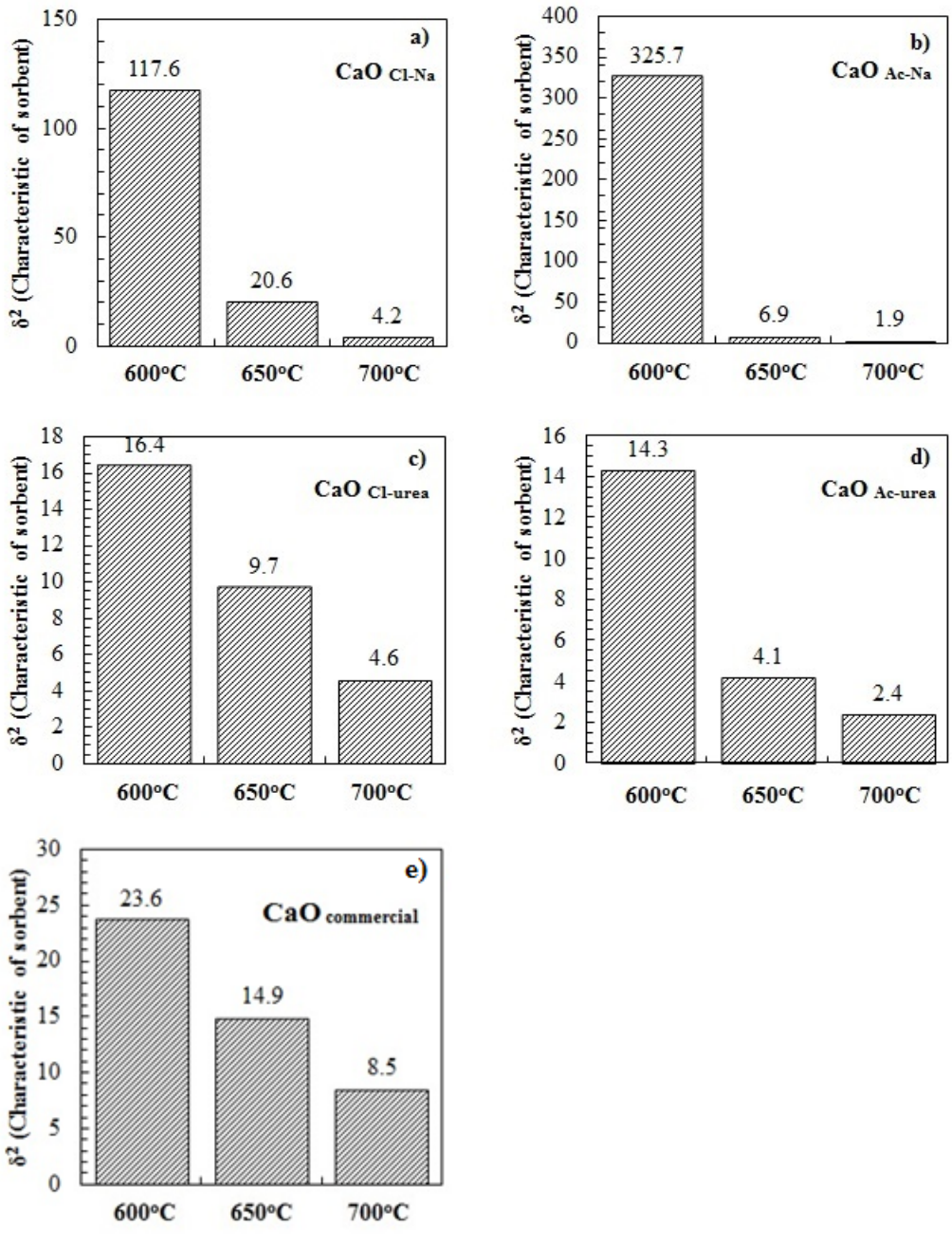

Fig. 7: Sorption behavior of CaO: a) $CaO_{Cl\text{-}Na}$, b) $CaO_{Cl\text{-}urea}$, c) $CaO_{Ac\text{-}Na}$, d) $CaO_{Ac\text{-}urea}$, and e) $CaO_{commercial}$.

$CaO_{Cl\text{-}Na}$ and $CaO_{Ac\text{-}Na}$ are found to adsorb low CO_2 capacity (0.14 gCO_2/gCaO) at 600°C due to low kinetic rate. With increasing temperature to at 650°C and 700°C, capacity of $CaO_{Cl\text{-}Na}$ and $CaO_{Ac\text{-}Na}$ largely increase. On the other hand, rate of increasing capacity of $CaO_{Cl\text{-}urea}$ is too low at elevated carbonation temperature because CO_2 might diffuse through layer of $CaCO_3$ of the small aggregated particles

found with $CaO_{Cl\text{-}Na}$ and $CaO_{Ac\text{-}Na}$ easier than the larger particles of $CaO_{Cl\text{-}urea}$. $CaO_{Ac\text{-}urea}$ shows good performances for CO_2 sorption because the morphology of CaO exhibits large network of connected small particles. The channels of porous on surface of CaO, which observed from SEM image (Fig. 5), would favor mass transfer (Florin and Harris, 2009) and hence promotes the ease accessibility of CO_2 to available surface active of CaO.

5.2 Effect of additive addition on properties of CaO-derived $CaCO_3$ and CO_2 sorption capacity

5.2.1 Characteristic of $CaCO_3$ sorbent

XRD patterns of $CaCO_3$ synthesized with the use of different concentrations of SDS surfactant is shown in Fig. 8. $CaCO_3$ synthesized with SDS surfactant at 10 mM and 20 mM, show aragonite phase, which is similar to the synthesized $CaCO_3$ without surfactant. $CaCO_3$ with the addition of 40 mM SDS surfactant occurs phase transfer from pure aragonite to the mixed phases of calcite (24%) and aragonite (76%).

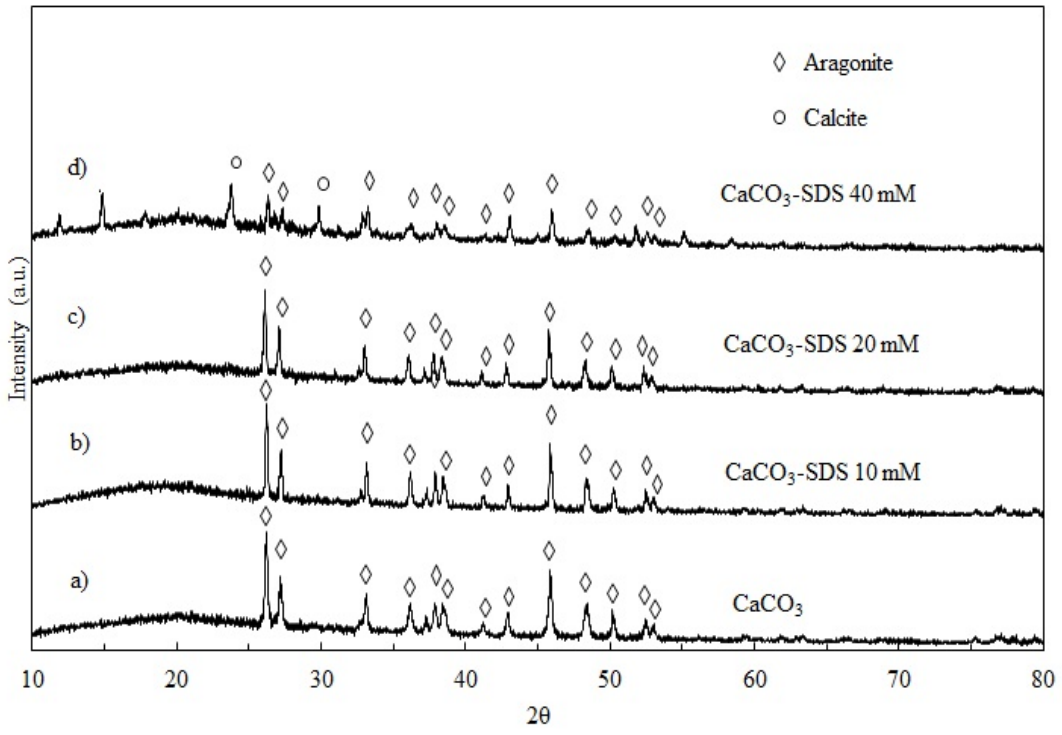

Fig. 8: XRD patterns of $CaCO_3$ with SDS surfactant at concentration a) without SDS, b) 10 mM, c) 20 mM, d) 40 mM.

For $CaCO_3$ synthesized with the addition of Gemini surfactant, XRD patterns indicate aragonite phase of $CaCO_3$ at 0.045 mM, which is similar to the synthetic $CaCO_3$ without surfactant. Adding Gemini surfactant at concentration of 0.08 mM, 0.12 mM, and 2 mM in precipitation shows phase of aragonite whereas 4 mM of Gemini surfactant induces the mixture of calcite (3%) and vaterite (97%) phase to form.

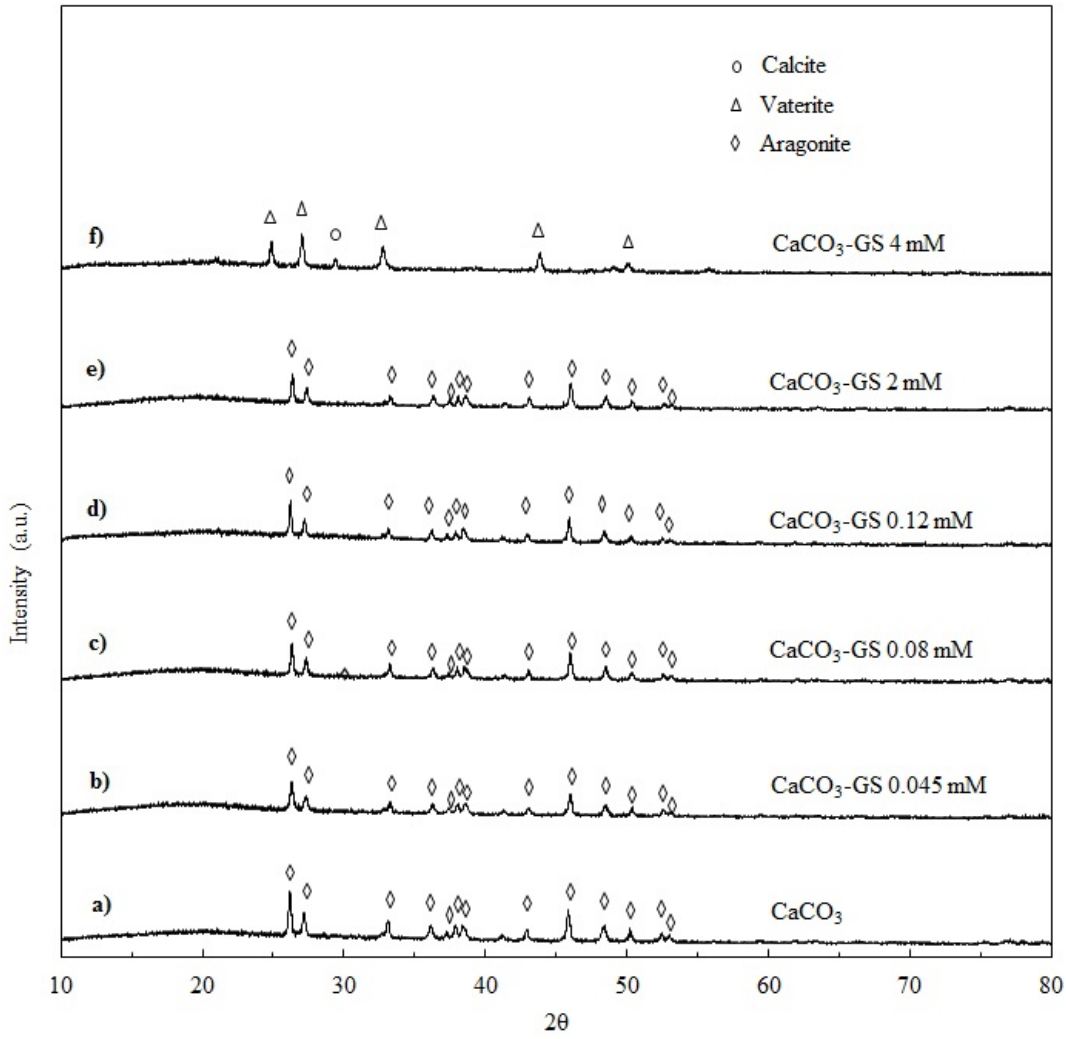

Fig. 9: XRD patterns of $CaCO_3$ with Gemini surfactant at concentration of a) without Gemini surfactant, b) 0.045 mM, c) 0.08 mM, d) 0.12 mM, e) 2 mM, f) 4 mM.

Morphologies of $CaCO_3$ sorbents observed by SEM are shown in Fig. 10. $CaCO_3$ without surfactant shows morphology of aggregated particles whereas $CaCO_3$ with surfactant presents rod-like structure with different particle sizes depend upon concentration used. Concentration of 10 and 20 mM of SDS surfactants offer rod-like

structure with average size particles of 3-5 μm. The rod shape of $CaCO_3$ is shorten to 1 μm and tends to aggregate into large particle when concentration of surfactant was increased to 40 mM.

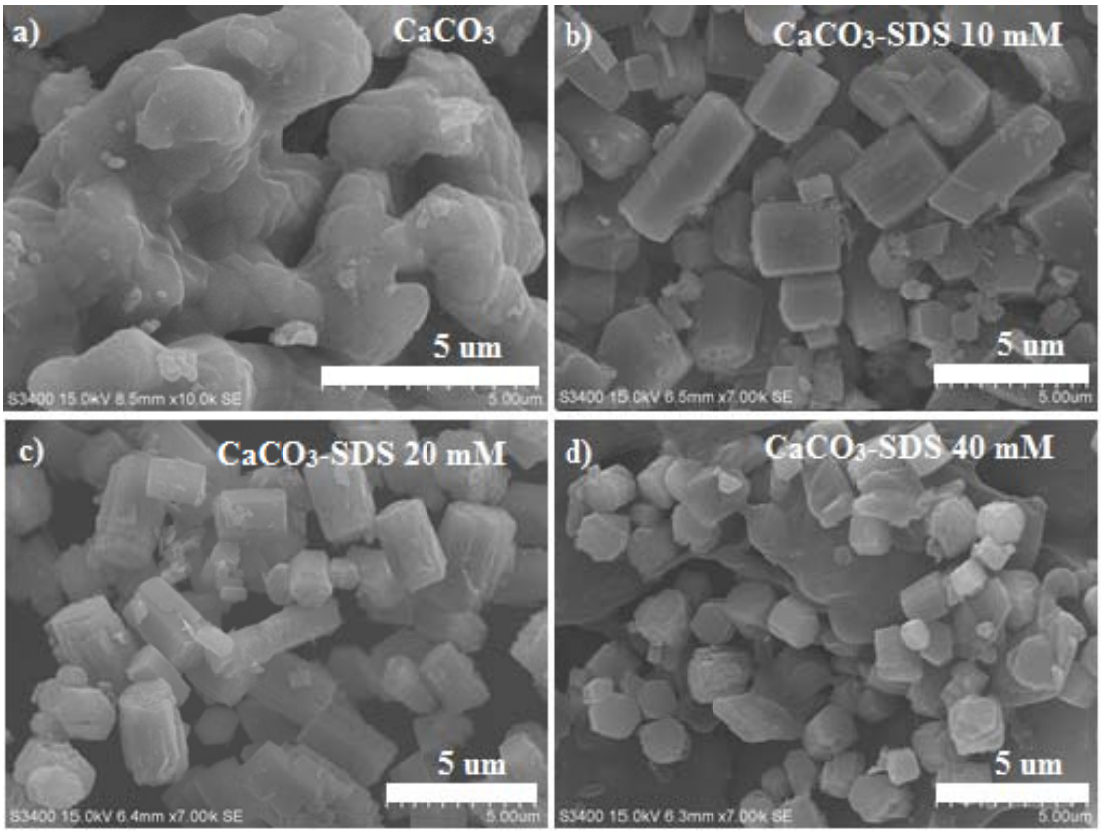

Fig. 10: SEM images of $CaCO_3$ with the addition of various concentrations of SDS a) without surfactant, b) 10 mM, c) 20 mM, d) 40 mM.

SEM images of $CaCO_3$ after synthesis with the addition of Gemini surfactant are shown in Fig. 11. The results of using Gemini surfactant as additive at 0.045 mM, 0.08 mM, and 0.12 mM show uniform needle-like structure. $CaCO_3$-GS 2 mM provides large needle-like, whereas 4 mM concentration of Gemini surfactant exhibits small particle aggregation.

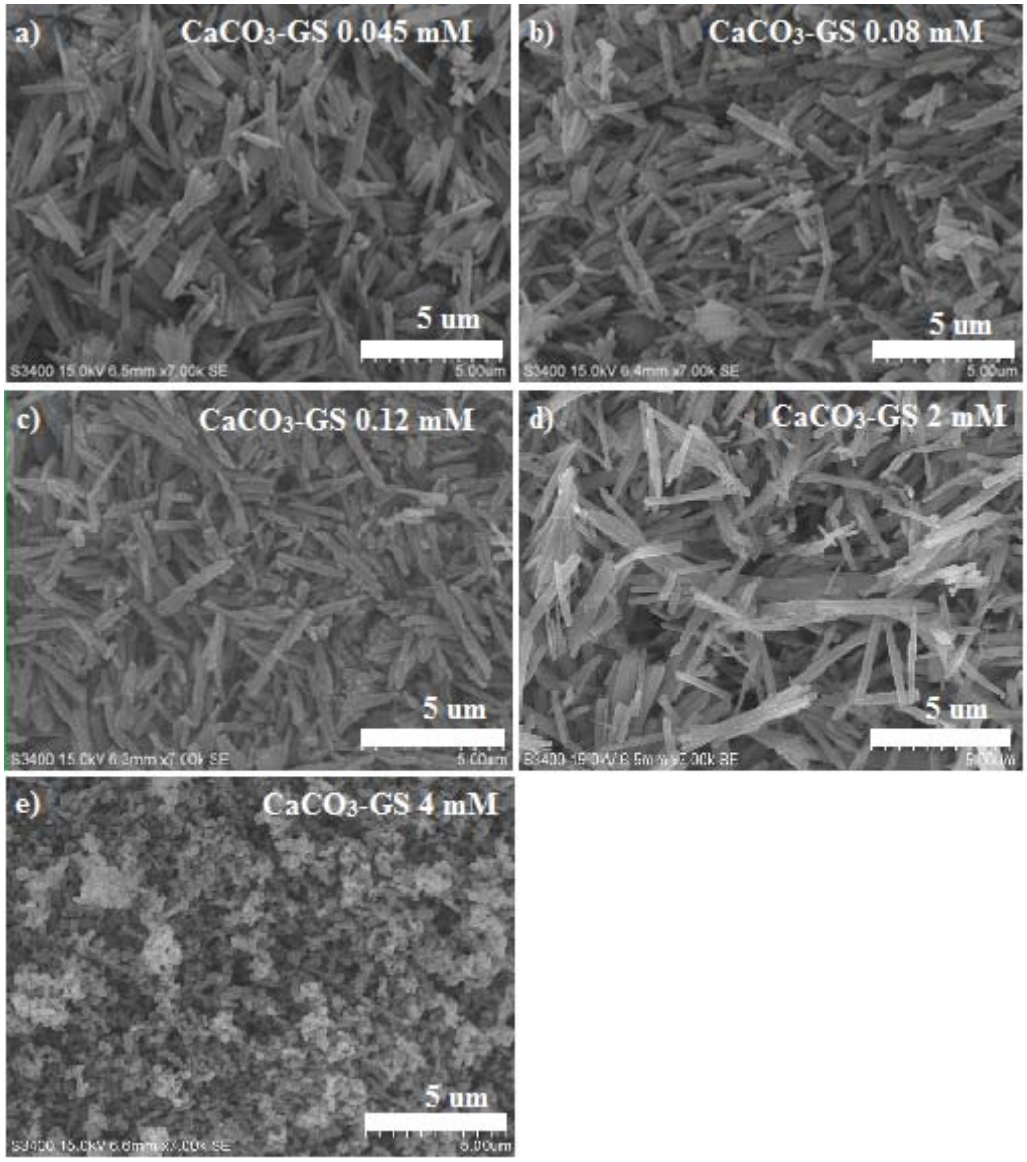

Fig. 11: SEM images of $CaCO_3$ synthesized with adding various concentrations of Gemini surfactant a) 0.045 mM, b) 0.08 mM, c) 0.12 mM, d) 2 mM, e) 4 mM.

Fig. 12 shows decomposition of $CaCO_3$ synthesized with the addition of SDS surfactant at concentrations of 10 mM, 20 mM, and 40 mM analyzed by TGA. The 10-mM $CaCO_3$-SDS and the 20-mM $CaCO_3$-SDS show one step decomposition of $CaCO_3$ at approximately 600-800°C, indicating the release of CO_2 as 40% weight loss of CO_2 is observed. The 40-mM $CaCO_3$-SDS exhibits weight loss at 220-450°C and 630-740°C, which indicates decomposition of SDS surfactant and CO_2 from $CaCO_3$. The presence of two decomposition temperature implies that surfactant might adsorb on surface of $CaCO_3$. The decomposition of $CaCO_3$ and SDS at all concentrations observed from DTA exhibits endothermic reaction of decomposition.

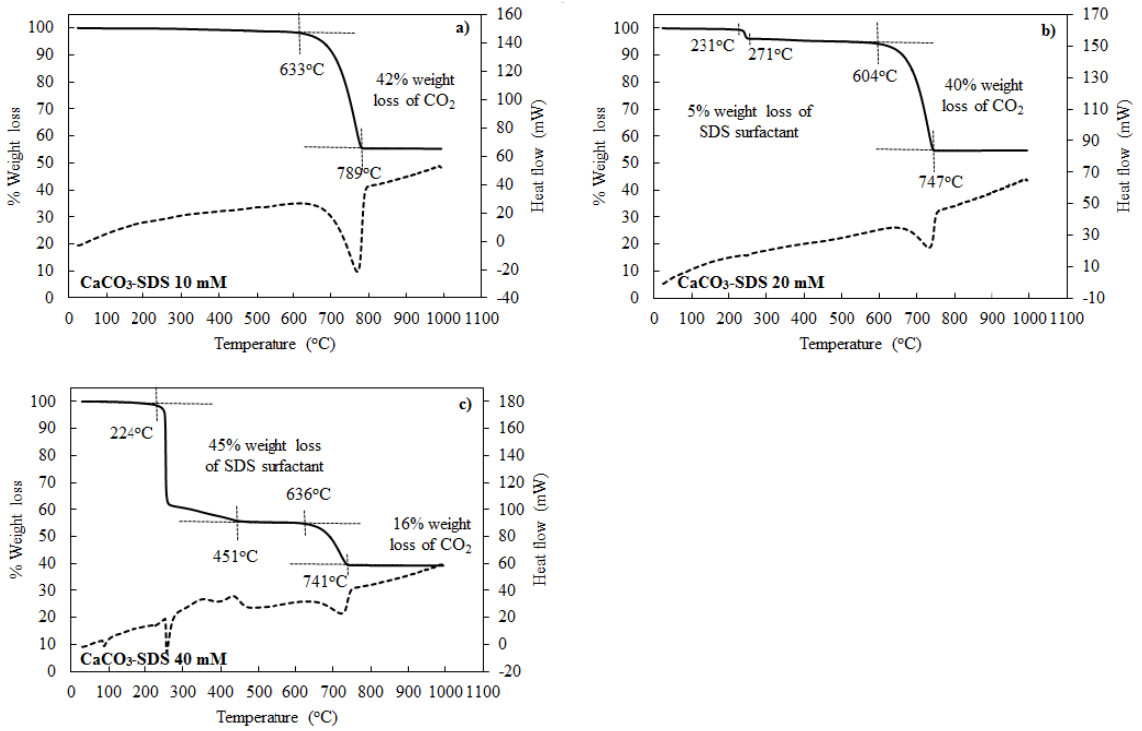

Fig. 12: TGA results of weight decomposition of $CaCO_3$ with SDS surfactant at a) 10 mM, b) 20 mM , c) 40 mM.

TGA results of $CaCO_3$ with Gemini surfactants using concentrations of 0.045 mM, 0.08 mM, 0.12 mM, 2 mM, and 4 mM are shown in Fig. 13. $CaCO_3$-GS 0.045 consists of two steps of decomposition, which might be weight loss of Gemini surfactant at 343-428°C and CO_2 from $CaCO_3$ at 571-702°C. For the other $CaCO_3$ sorbents: $CaCO_3$-GS 0.08 mM, 0.12 mM, 2 mM, and 4 mM, 44% weight loss are found at 600-800°C, which indicates the release of CO_2. DTA results show endothermic reaction of decomposition of Gemini surfactant and $CaCO_3$ in both temperature ranges of 350-450°C and 500-700°C, respectively. The $CaCO_3$ were completely decomposed to CaO at temperatures higher than 800°C.

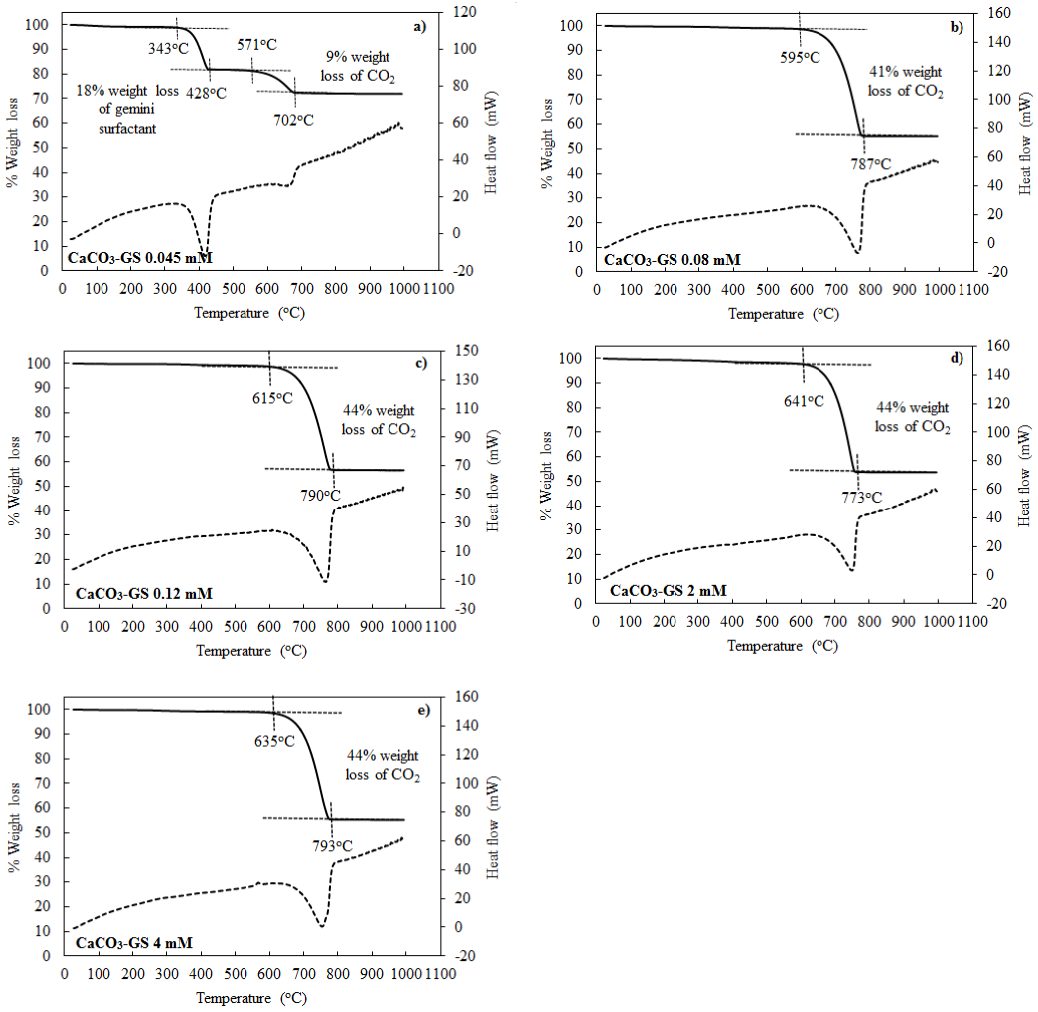

Fig. 13: TGA results of weight decomposition of $CaCO_3$ with adding Gemini surfactant at a) 0.045 mM, b) 0.08 mM, c) 0.12 mM, d) 2 mM, e) 4 mM.

Fig. 14 and Fig. 15 show XRD patterns of CaO obtained from the calcination of $CaCO_3$ synthesized with the use of SDS surfactant and Gemini surfactant. The pattern of all CaO samples exhibit major peaks at 2θ of 32.2, 37.4, 53.9, 64.2, and 67.4°, indicating the complete decomposition of $CaCO_3$ to CaO.

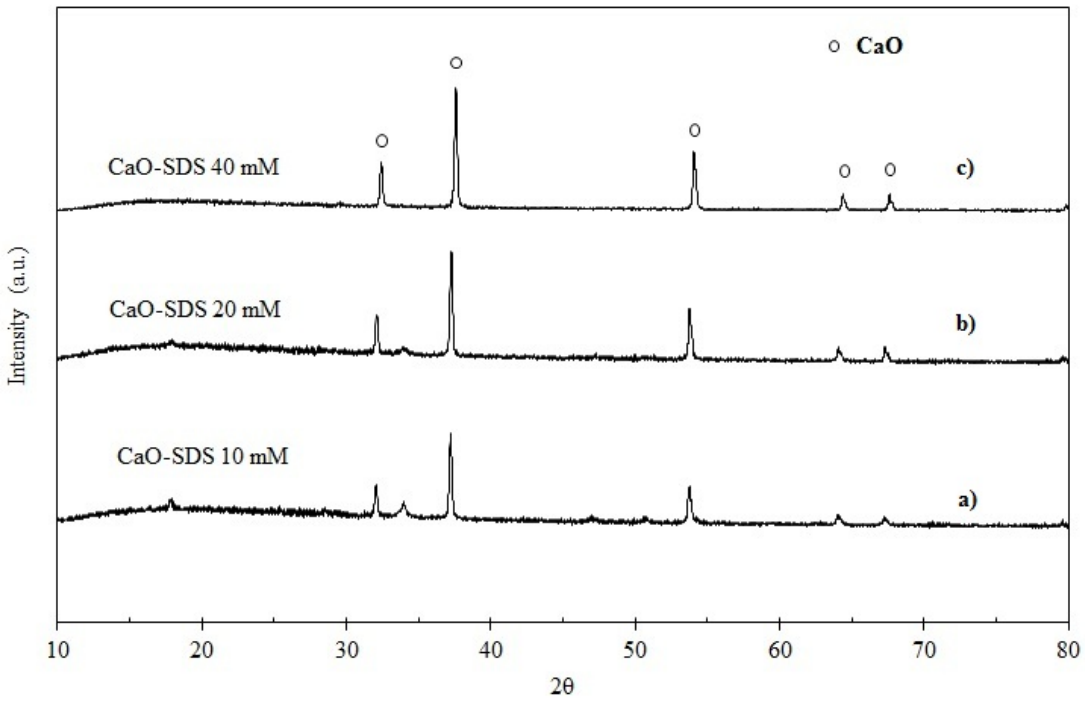

Fig. 14: XRD patterns of CaO with the addition of SDS surfactant at concentration a) 10 mM, b) 20 mM, d) 40 mM.

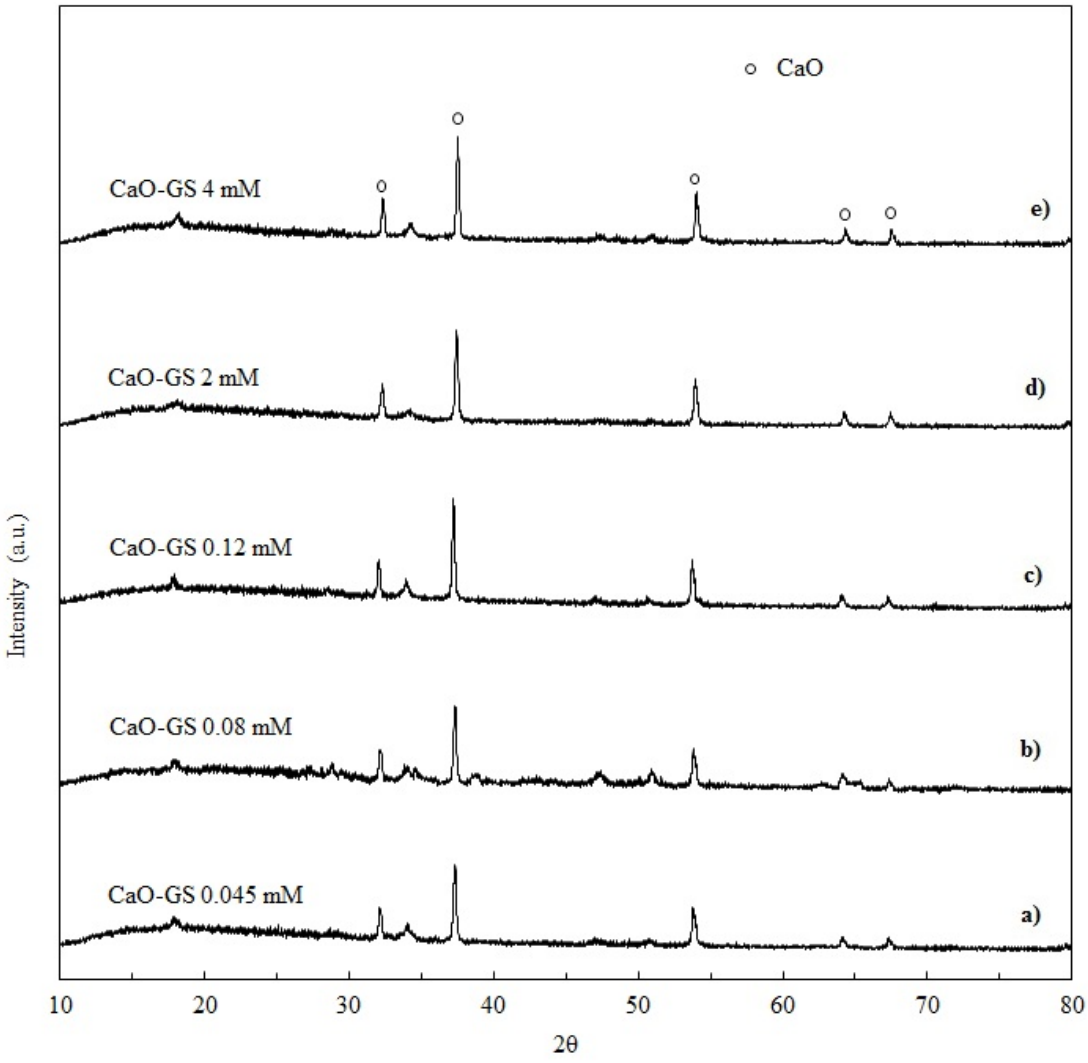

Fig. 15: XRD patterns of CaO with the addition of Gemini surfactant at concentration a) 0.045 mM, b) 0.08 mM, c) 0.12 mM, d) 2 mM, e) 4 mM.

Morphologies of CaO derived from $CaCO_3$ synthesized with the use of SDS obtained by SEM photographs are shown in Fig 16. CaO with 10 mM of SDS surfactant has oval-like morphology with rough surface and average size of 2-5 μm. CaO with the addition of 20 mM and 40 mM of SDS show agglomeration of small particles.

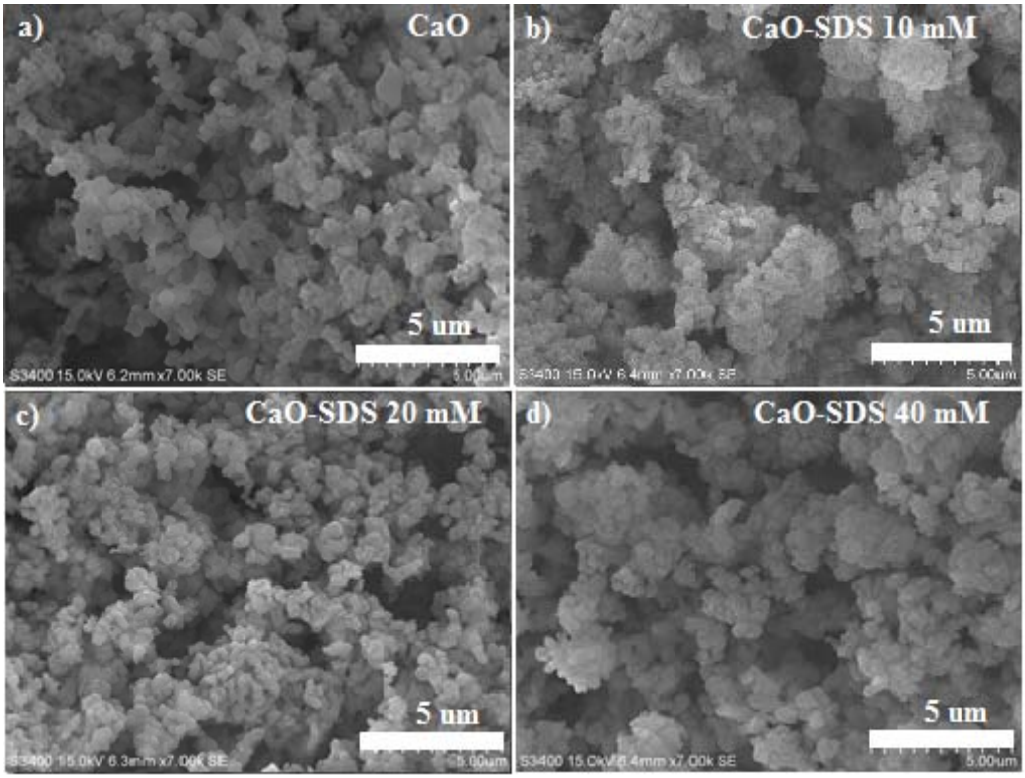

Fig. 16: SEM images of CaO at various concentrations of SDS a) without surfactant, b) 10 mM, c) 20 mM, d) 40 mM.

Fig. 17 exhibits morphologies of CaO obtained from $CaCO_3$ synthesized with the addition of Gemini surfactant. CaO with adding Gemini surfactant of 0.045 mM has aggregation of smooth particles. Increasing concentration of Gemini surfactant leads to small aggregated particles.

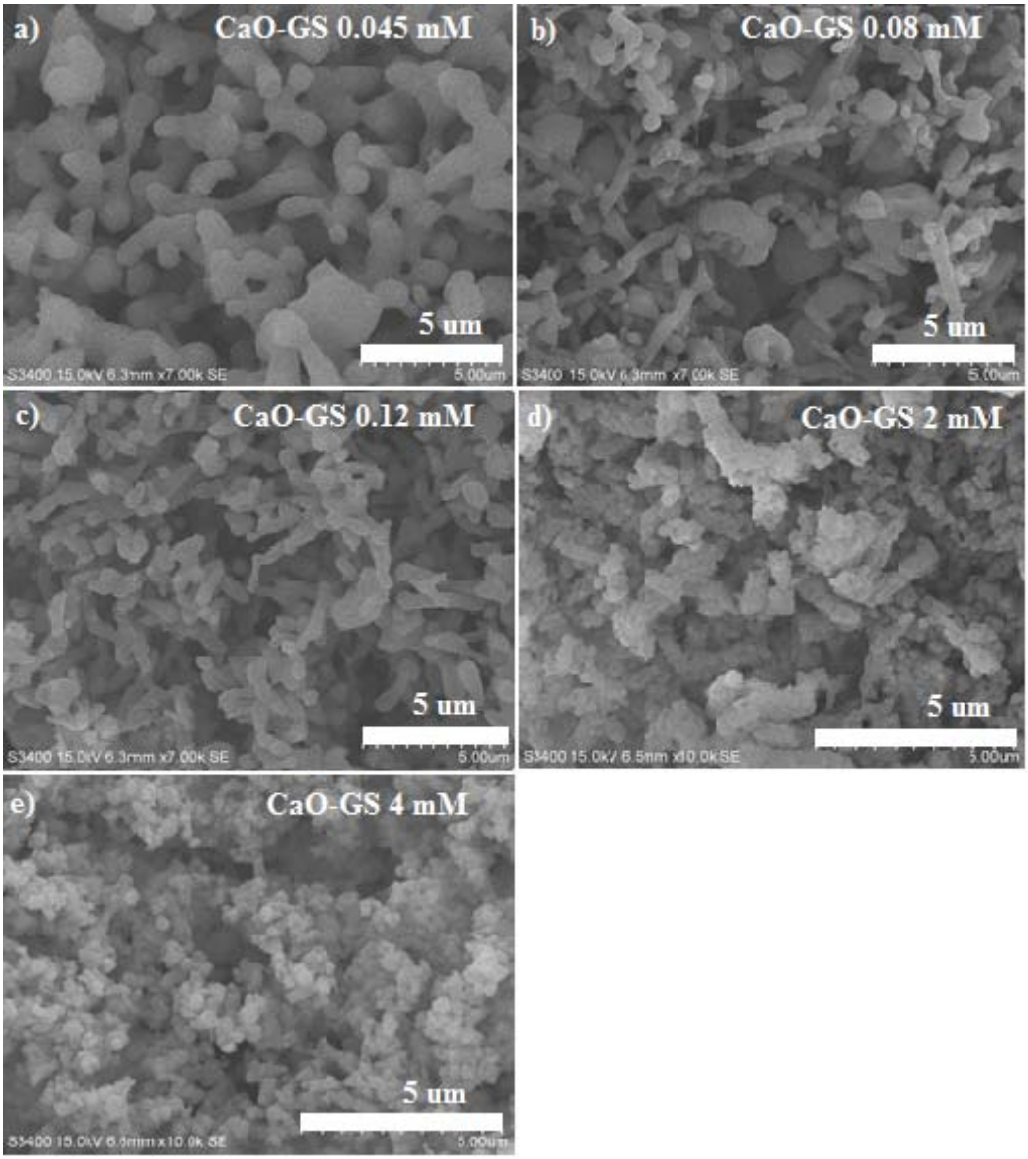

Fig. 17: SEM images of CaO with the addition of various concentrations of Gemini surfactant a) 0.045 mM, b) 0.08 mM, c) 0.12 mM, d) 2 mM, e) 4 mM.

Crystal size of CaO was calculated by Scherrer equation at the highest peak of CaO of 37.4° as shown in Table 5. CaO with adding SDS surfactant has similar crystallite size to CaO without surfactant; however, the Gemini surfactant offers lower crystallite size of CaO when compared to those without surfactants and those with the addition of SDS surfactant. Textural properties such as surface area, pore volume, and pore diameter of CaO synthesized with the addition of surfactant at different concentrations are also shown in Table 5. The BET surface area of CaO synthesized with the use of SDS surfactant is lower than that without surfactant whereas CaO synthesized with adding Gemini surfactant possess higher BET surface area than others.

Table 5: Textural properties of CaO sorbents synthesized with/without the addition of surfactants

Sample	Surface area (m^2/g)	Pore volume (cm^3/g)	Pore size diameter (nm)	Crystal size
CaO	9.8	0.063	27.5	44.3
CaO-SDS 10 mM	7.6	0.026	14.1	45.0
CaO-SDS 20 mM	9.4	0.036	15.0	44.0
CaO-SDS 40 mM	1.7	0.004	9.9	40.4
CaO-GS 0.045 mM	12.1	0.138	45.6	37.8
CaO-GS 0.08 mM	14.9	0.084	22.6	37.9
CaO-GS 0.12 mM	14.6	0.063	17.4	37.7
CaO-GS 2 mM	16.3	0.059	14.5	37.6
CaO-GS 4 mM	12.9	0.097	30.2	41.1

5.2.2 CO_2 sorption tests

CaO sorbents, which improved by adding SDS surfactant at different concentrations, were tested for CO_2 adsorption at 600°C. The results in Fig. 18 show that adding SDS surfactant have an effect on CO_2 sorption capacity and the ability of the adsorption also depend upon concentration of surfactant used. The CaO synthesized without SDS shows 20% conversion. When SDS was added at 10 mM and 20mM, conversion of CaO increases to 32% and 34%, respectively. In contrast, conversion of CaO decreases to 19% when concentration of SDS was further increased to 40 mM. Lower CaO conversion observed with the 40 mM-SDS might be due to CaO particles were aggregated, resulting in low surface area (1.7 m^2/g). Maximum CaO conversion of 34% is observed with CaO-SDS 20 mM.

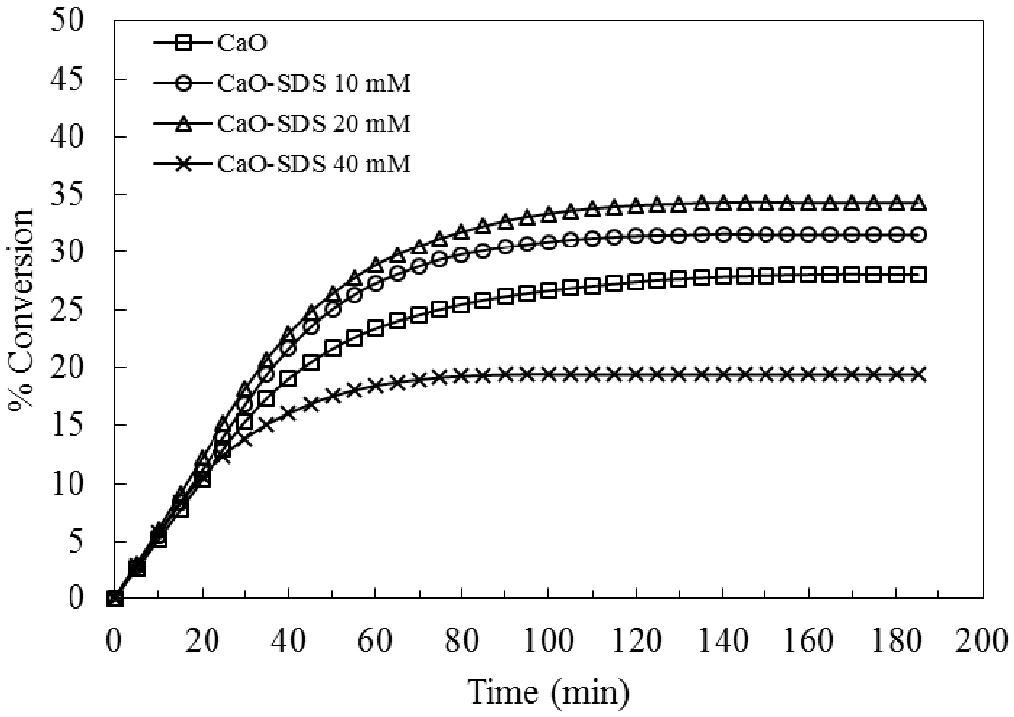

Fig. 18: Conversion of CaO synthesized without and with adding SDS surfactant at concentration 10 mM, 20 mM, 40 mM.

Fig. 19 shows conversion of CaO synthesized with the use of Gemini surfactant at various concentrations. The CaO with small amount of Gemini surfactant added, 0.045 mM, 0.08 mM, 0.12 mM, obtained relative conversion of 30% and the conversion increases to 37% when Gemini surfactant was increased to 2 mM. Conversely, CaO-GS 4 mM exhibits low conversion of 20%.

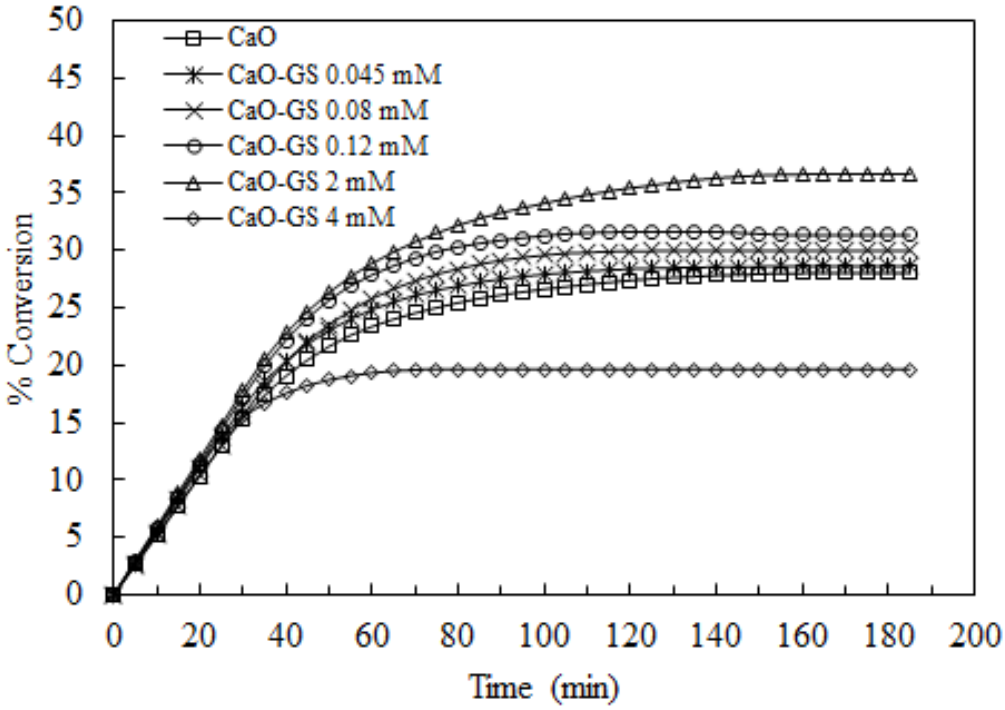

Fig. 19: Conversion of CaO synthesized without and with adding Gemini surfactant at concentration 0.045 mM, 0.08 mM, 0.12 mM, 2 mM, 4 mM.

Fig. 20 summarizes CO_2 sorption capacity adsorbed by different CaO sorbents. CaO-SDS 10 mM and CaO-SDS 20 mM exhibit capacity of 0.25 and 0.27 gCO_2/gCaO, respectively, the value of which is closed to CO_2 sorption capacity of CaO without surfactant. In contrast, CO_2 sorption capacity of CaO-SDS 40 mM has the lowest sorption capacity of 0.18 gCO_2/gCaO because the sorbent has low surface area (1.7 m^2/g) and dense structure as shown in Table 2 and Fig 16, respectively.

CaO sorbents with the addition of Gemini surfactant with concentrations of 0.045 mM, 0.08 mM, and 0.12 mM show sorption capacity of 0.22, 0.24, and 0.25 gCO_2/gCaO, respectively. Maximum sorption capacity observed with 2 mM of adding Gemini surfactant might be due to the highest BET surface area of 16.3 m^2/g. CaO-GS 2 mM shows capacity of 0.29 gCO_2/gCaO, whereas CaO-GS 4 mM has capacity of 0.15 gCO_2/gCaO because high concentration of Gemini surfactant (4 mM) promotes agglomeration of particles.

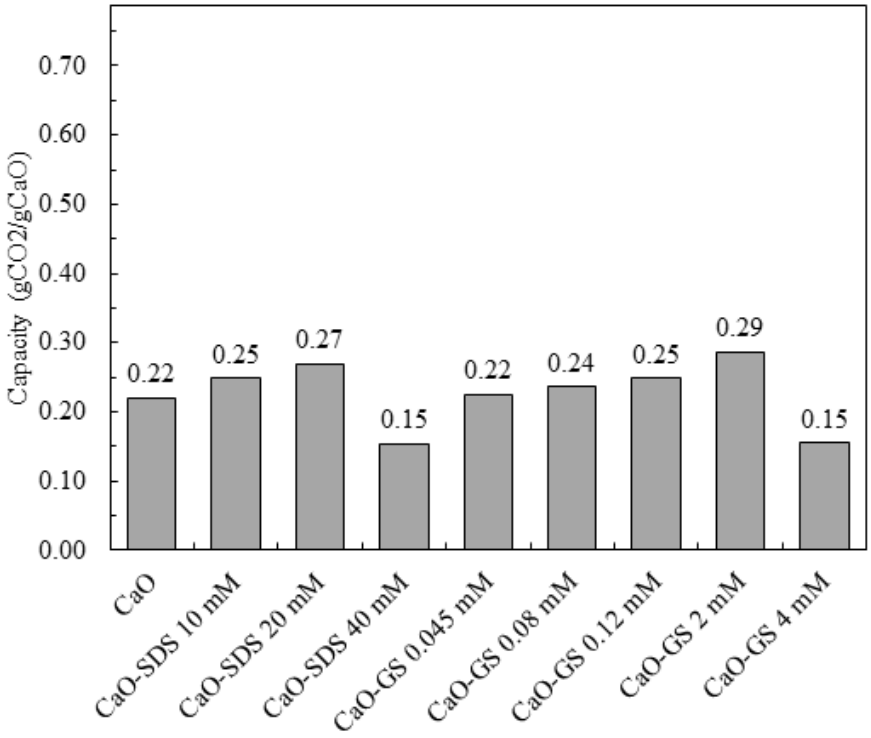

Fig. 20: Capacity of CaO with the addition of surfactants.

5.2.3 Proposed mechanism of surfactant on structure of $CaCO_3$

Surfactant additives, SDS and Gemini surfactants, are consisted of anionic head group $-SO_3^-$ group. At critical micelle concentration (CMC), SDS forms rod-like micellar structure whereas needle-like is formed in case of Gemini surfactant.

$CaCO_3$ without surfactant shown agglomeration of particles as depicted in Fig. 10, when SDS surfactant was added into the system, the particles was separated and the $CaCO_3$ morphology was controlled to shape rod-like structure by SDS surfactant. The results of TGA (Fig. 12) can indicate adsorption of SDS surfactant on $CaCO_3$. The SDS micelle at 10 mM and 20 mM might be adsorbed on surface of $CaCO_3$ as shown in Fig 21. $CaCO_3$ with 40 mM shows small cubic and agglomeration that might be due to large amount of SDS surfactant is sufficient to direct particles to form small cubic and induce particles to aggregate. Proposed mechanism of the role of SDS surfactant to act as structure directing agent is shown in Fig. 21.

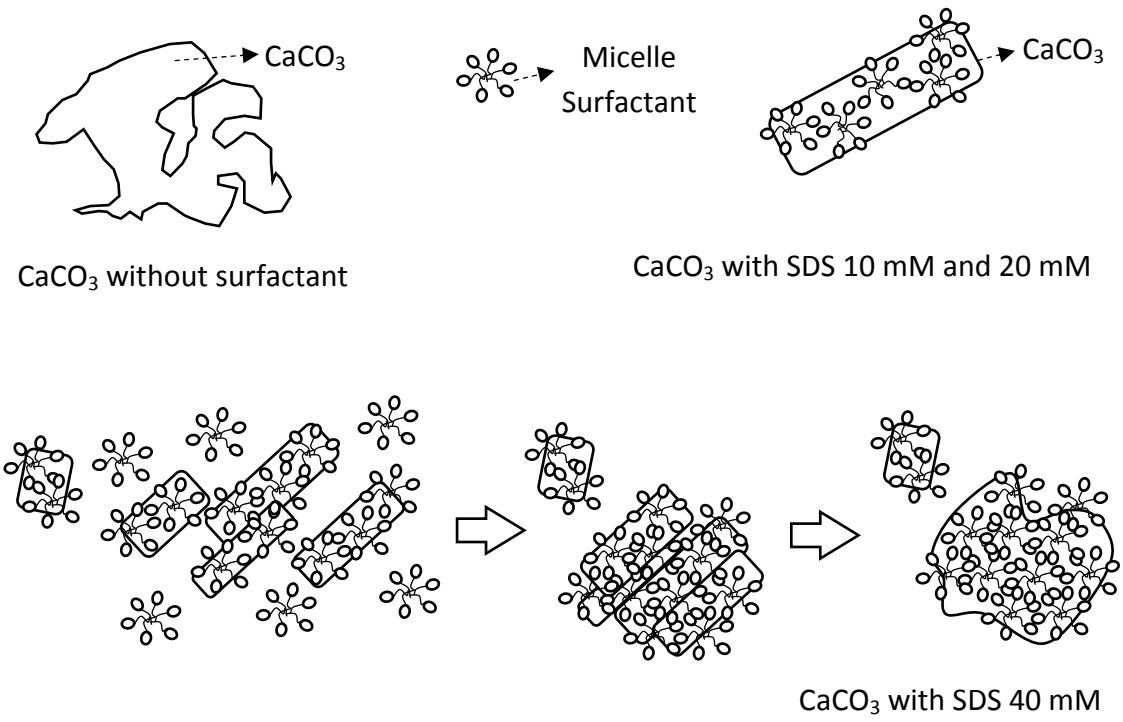

Fig. 21: Proposed mechanism of SDS at 10 mM 20 mM and 40 mM on $CaCO_3$ structure.

$CaCO_3$ sorbents with Gemini surfactant show different structures depend upon the concentration of Gemini added as shown in Fig. 11. The needle-like morphology observed with adding low concentration of Gemini surfactant (0.045 mM) might be occur from the lamellar formation of Gemini surfactant. When concentration was increased to 0.08-2 mM, larger particle of $CaCO_3$ is observed. This might be due to the result of self-interaction among Gemini surfactant molecules leading to the lowering between Gemini surfactant and $CaCO_3$. At 4 mM of Gemini surfactant, morphology of ellipse small particles is observed, which could be due to the control by complex ellipse micelle structure.

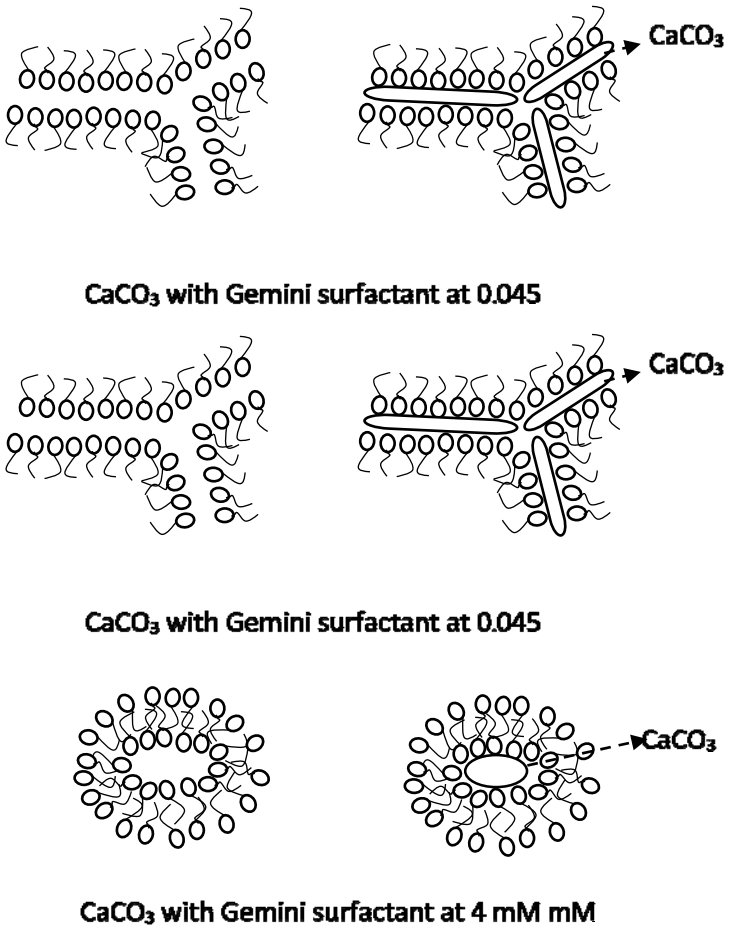

Fig. 22: Proposed mechanism of Gemini surfactant at 0.045 mM, 0.08 mM, 0.12 mM, 2 mM, and 4 mM on $CaCO_3$ structure.

5.3 Effect of metal incorporation on sorbent stability

5.3.1 Characteristic of CaO-based alumina sorbent

CaO-based alumina sorbents synthesized by different methods including wet mixing, co-precipitation, sol-gel, and sol mixing, were characterized by XRD as shown in Fig. 23. All of sorbents that synthesized by different methods show major peaks of CaO at 2 θ of 32.2, 37.4, 53.9, 64.2, and 67.4. The CaO-based sorbent, which were synthesized by sol mixing, wet mixing-GS 2 mM, co-precipitation, and co-precipitation-GS 2 mM, provide CaO and $Ca_{12}Al_{14}O_{33}$. The pattern of $Ca_{12}Al_{14}O_{33}$ exhibit at 2 θ of 18.0, 29.8, 33.2, 36.4, 40.9, 46.4, 54.9, and 57.2. Preparation by sol-gel and sol-gel-GS 2 mM show XRD pattern of CaO and $Ca_9Al_6O_{18}$. The pattern of $Ca_9Al_6O_{18}$ show peak of 2θ at 33.2, 47.7, and 60.0. Formation of calcium alumina complex occurred from diffusion of CaO into Al_2O_3. The presence $Ca_9Al_6O_{18}$ in sol-gel method occurred from Ca^{2+} can continue to diffuse into $Ca_{12}Al_{14}O_{33}$, which might be due to this method is release high energy from combustion reaction (Zhou et al., 2012). Formation of $Ca_{12}Al_{14}O_{33}$ is occurred from reaction of CaO with Al_2O_3 at high temperature (more than 800°C). In addition, absence calcium aluminate complex might be occurred from diffusion resistant of CaO into Al_2O_3 prevent conversion of calcium aluminate complex, resulting in the presence of CaO and Al_2O_3 in XRD patterns.

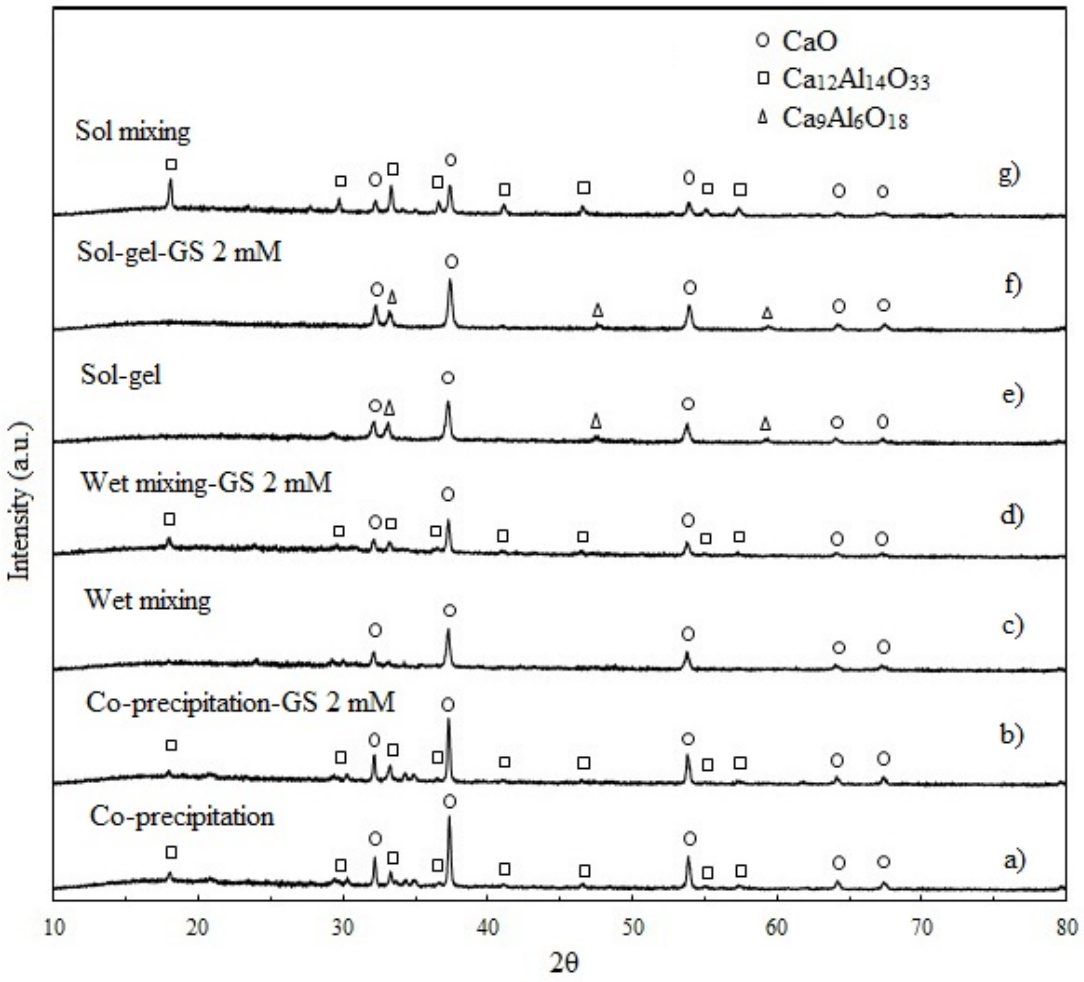

Fig.23*:* XRD of CaO-based sorbent that synthesized by several methods*:* a*)* Co-precipitation, b*)* Co-precipitation-GS 2 mM, c*)* Wet mixing, d*)* Wet mixing-GS 2 mM, e*)* Sol-gel, f*)* Sol-gel-Gs 2 mM, and g*)* Sol mixing.

Morphologies of CaO-based sorbent observed from SEM images are shown in Fig. 24. Sorbent from wet mixing obtained large particle and rough surface; however, when Gemini surfactant was added the particle of sorbent becomes agglomerated with rough surface. Aggregation of particles and rough surface are also found with the sorbents synthesized by co-precipitation: rough surface is observed with the sorbent without surfactant whereas slit on surface is observed with co-precipitation-GS 2 mM. Sorbent, which is synthesized by sol-gel method formed uniform small particles with particle size of 1-2 μm. The particles of CaO-based prepared by sol-gel with Gemini surfactant 2 mM tend to agglomerate than the sorbent without surfactant. Structure of sorbent, which is prepared by sol mixing, shows aggregation of large particles (4-5 μm) and small particles (1-2 μm).

Distribution of calcium and aluminum on CaO-based alumina sorbent was observed by SEM-EDX as shown in Fig. 25. All sorbents exhibit uniform dispersion of calcium an aluminum.

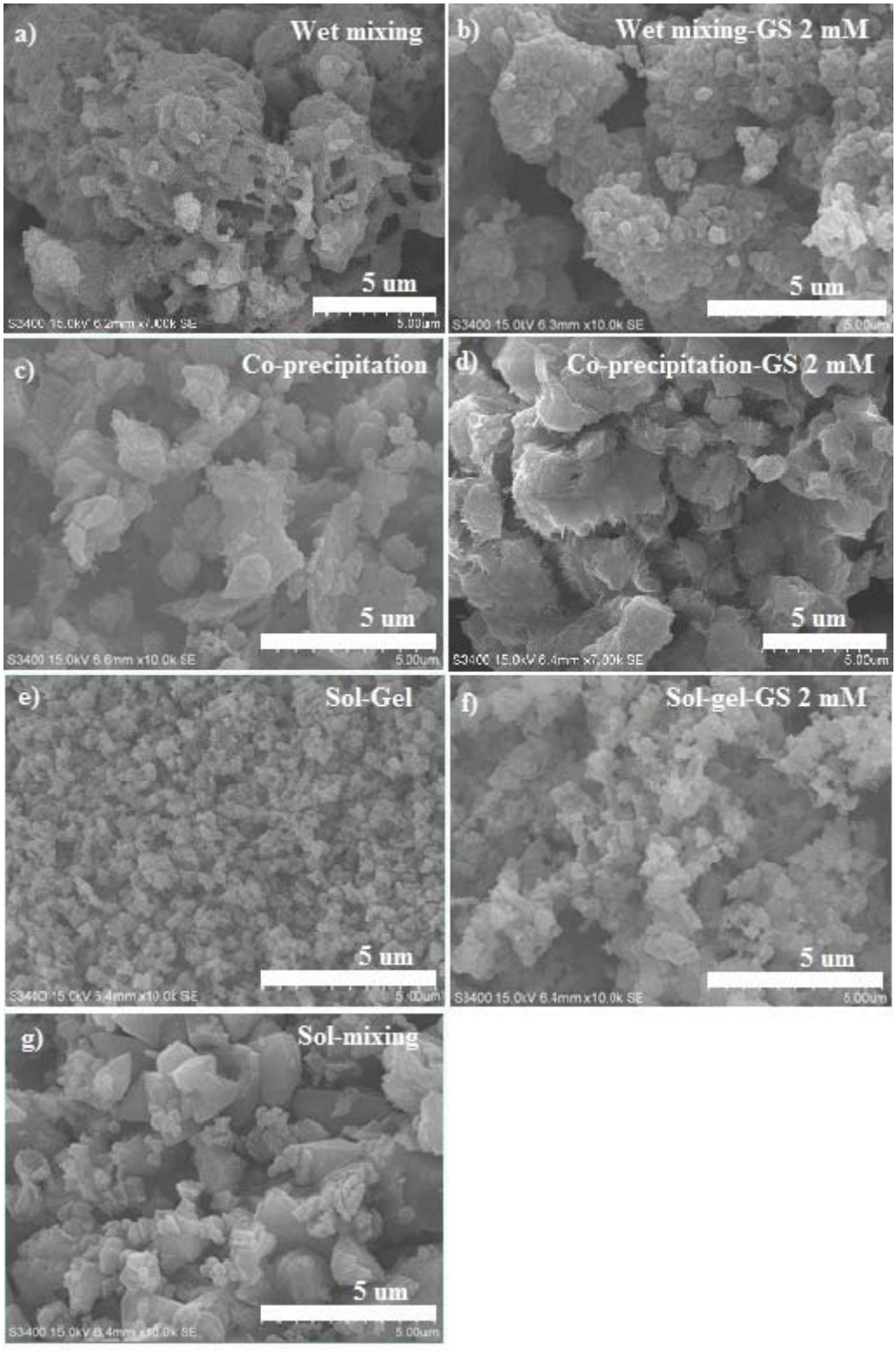

Fig. 24*:* SEM image of CaO-based sorbent synthesized from several methods*:* a*)* wet mixing, c*)* co-precipitation, e*)* sol-gel, and g*)* sol-mixing, and CaO-based sorbent from addition additive*:* b*)* wet mixing-GS 2 mM, d*)* co-precipitation-GS 2 mM, and f*)* sol-gel-GS 2 mM**.**

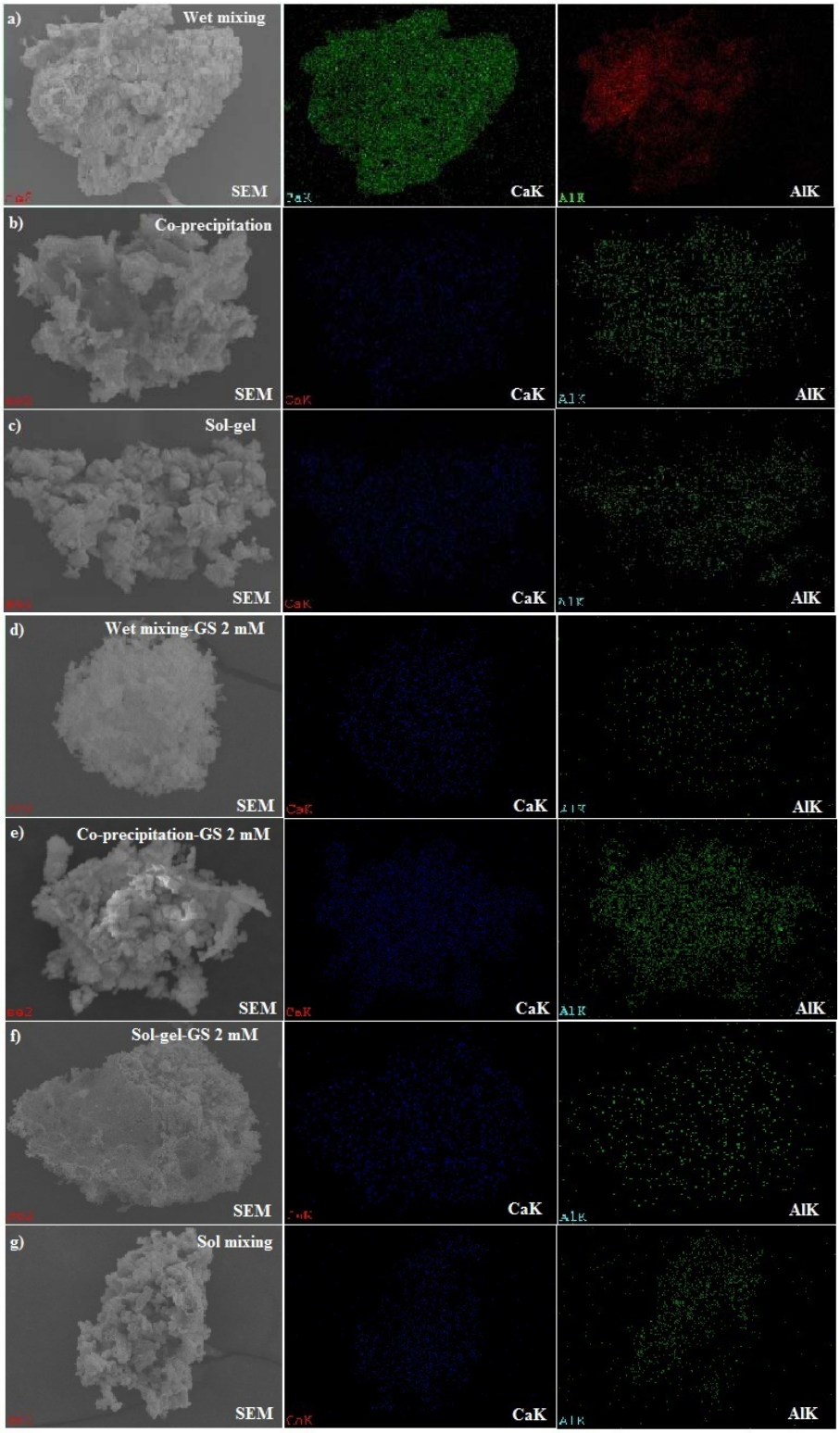

Fig. 25*:* SEM-EDX of calcium and aluminum synthesized by a*)* wet mixing, b*)* co-precipitation, c*)* sol-gel, d*)* wet mixing-GS 2 mM, e*)* co-precipitation-GS 2 mM, f*)* sol-gel-GS 2 mM and g*)* sol mixing**.**

The ratio of calcium and aluminum of each sorbent determined by hydration and TGA technique are shown in Table 6.

Table 6: Composition at surface of sorbent by hydration method

Samples	%CaO ($TGA_{Decomposition}$)
Wet mixing	73
Co-precipitation	47
Sol-gel	65
Wet mixing-GS 2 mM	70
Co-precipitation-GS 2 mM	64
Sol-gel-GS 2 mM	77
Sol-mixing (GS 2 mM)	64

Table 7 presents textural properties including surface area, pore volume, and pore size distribution of CaO-based alumina synthesized from different synthesis methods. CaO-based sorbents, which were synthesized with Gemini surfactant, obtained low surface area than those without surfactant. These results indicate that addition of Gemini surfactant promotes agglomeration of particles, leading to a decrease in surface area.

Table 7: Textural properties of CaO-based sorbents.

Sample	Surface area (m^2/g)	Pore volume (cm^3/g)	Pore size diameter (nm)
Wet mixing	8.8	0.040	18.1
Co-precipitation	2.2	0.033	58.6
Sol-gel	8.4	0.067	31.5
Wet mixing-GS 2 mM	4.3	0.108	100.7
Co-precipitation-GS 2 mM	1.7	0.0035	8.42
Sol-gel-GS 2 mM	8.0	0.060	29.7
Sol-mixing (GS 2 mM)	0.9	0.003	10.7

5.3.2 CO_2 sorption test

Ability of CaO-based alumina sorbents synthesized with/without surfactant by different methods on CO_2 sorption shown as conversion is demonstrated in Fig. 26. Magnitude of CaO conversion of different sorbents is in the order: sol-gel > wet mixing > co-precipitation. The different in CO_2 sorption ability found with different methods could be due to difference in structures, small particle from sol-gel provides good performance than large particles with rough surface obtained from co-precipitation and wet mixing. Large compact particles obtained from co-precipitation offers the lowest sorption capacity.

Adding Gemini surfactant does not affect conversion of the sorbent synthesized by wet mixing method where 18% conversion is maintained. However, when surfactant was added, conversion of Co-precipitation-GS 2 mM increases to 33%. This result might be due to the slit on surface of the sorbent. In contrast, conversion of the sol-gel-GS 2 mM decreases from 52% to 27% when compared with sol-gel. This might be because Gemini surfactant induces particles to agglomerate as shown by SEM results. Sol-mixing method shows the lowest conversion of 15%, which is due to the lowest surface area (0.9 m^2/g) and dense aggregated particles. The capacity of CO_2 sorption compared in unit of gram of CO_2 per gram of CaO content are shown in Fig. 27. The capacity is in the order: sol-gel >

co-precipitation-GS 2 mM > sol-gel-GS 2 mM > co-precipitation > wet mixing ~ sol mixing.

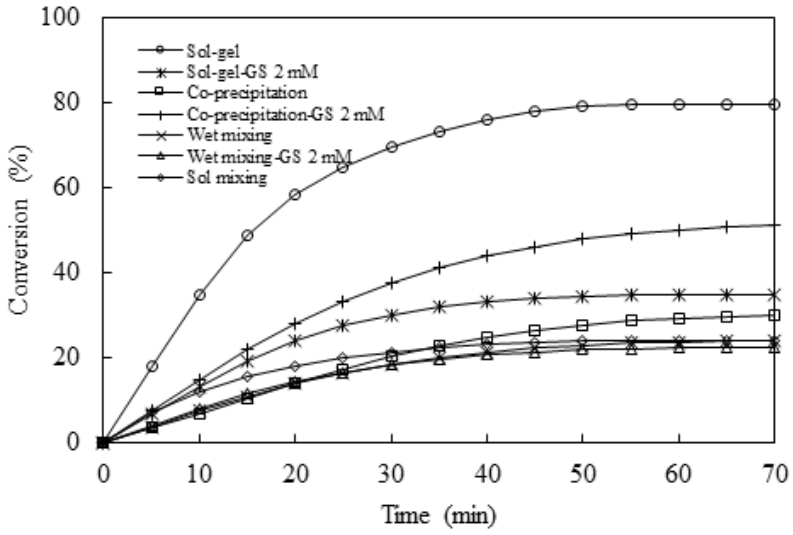

Fig. 26: Conversion of different CaO-based alumina sorbents.

Comparison between the sorbents with/without 2 mM of Gemini surfactant, wet mixing and sol mixing techniques show similar morphology between both sorbents and comparative sorption capacity of 0.20 gCO_2/gCaO, implying that the Gemini surfactant does not affect on properties of CaO-based sorbent. For co-precipitation technique, the sorbent with the addition of Gemini surfactant possess slit on surface. This could be a reason to enhance CO_2 sorption capacity due to an increase of an accessible active surface. CaO-based with Gemini surfactant, prepared by sol-gel, show agglomeration of particles that influenced on a decreasing of sorption capacity.

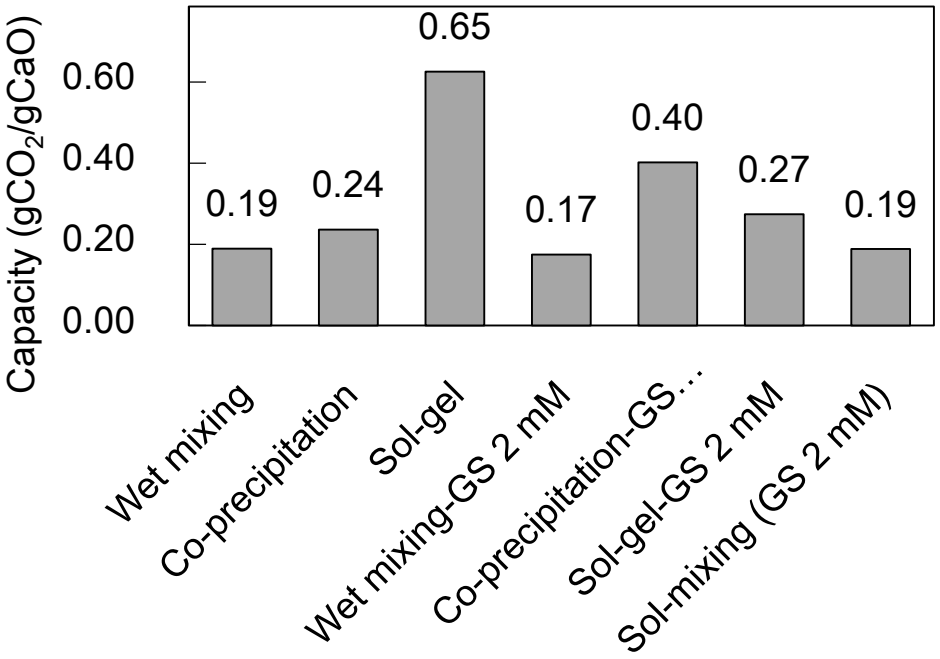

Fig. 27*:* Sorption capacity of different CaO-based sorbents**.**

The CaO-based sorbent prepared by sol-gel technique, which shows the highest capacity of CO_2 sorption, was further investigated its performance for multiple-cycle used as shown in Fig**.** 28**.** The results reveal that capacity of 0**.**65 gCO_2/gCaO observed in the 1st cycle decreases to 0**.**41 gCO_2/gCaO in the 10th cycle, which is considered as 36**%** reduction**.** Our results are comparable to that reported by Broda et al. (2012) whose the synthesized CaO-based by sol-gel method that contained 90**%**CaO and $Ca_{12}Al_{14}O_{33}$ showed a reduction of 22**%** sorption capacity in the 10th cycle**.** This result shows that by incorporating CaO with Al_2O_3 can improve properties of the sorbent in term of stability**.** Comparing to commercial CaO reported by Li et al. (2009), our sorbent exhibit much higher capacity than the commercial CaO which average particle of ~10μm (0.4gCO_2/gCaO) and similar to a commercial CaO very fine powder (160 nm) of 0.65gCO_2/gCaO in 1st cycle. However, our sorbent is inferior in term of 10th cycle stability comparing to the 160 nm CaO fine powder.However, our sorbent is inferior in term of 10th cycle stability comparing to the 160 nm CaO fine powder.

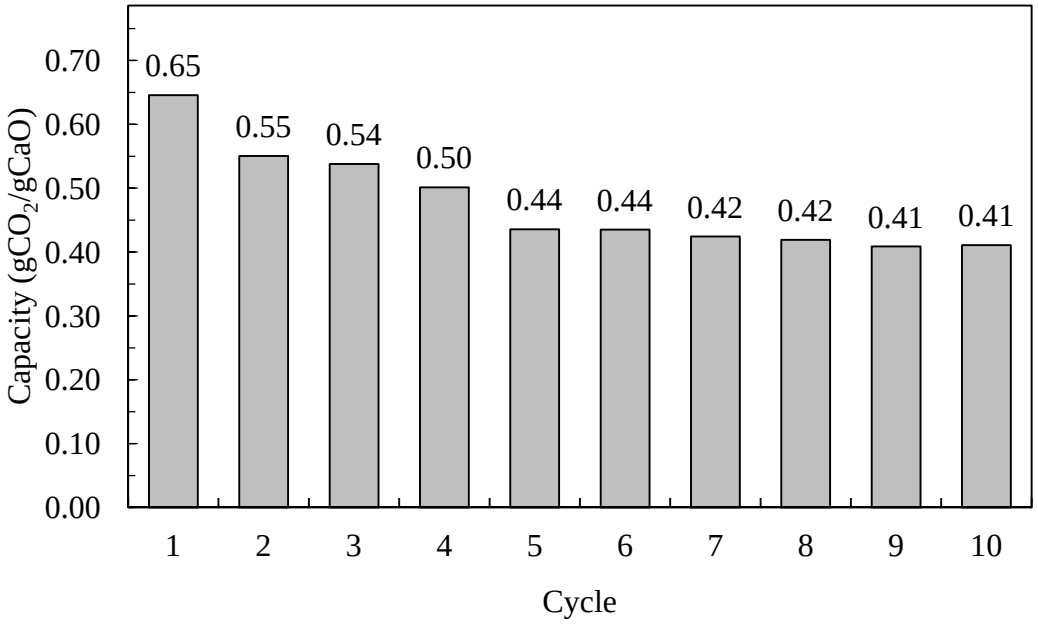

Fig. 28*:* CO_2 sorption capacity of CaO-based sorbent synthesized by sol-gel method repeated for 10^{th} cycles.

6. Conclusions

This work is attempted to improve properties of CaO-based sorbent for high-temperature CO_2 sorption. Results obtained from the study are summarized as follows.

1. Precipitation of $CaCO_3$ by using different precursors exhibits different morphologies, structures and have effect on morphology of CaO sorbent as well as the ability to adsorb CO_2. The large network of connected particles obtained from $CaO_{Ac\text{-}urea}$ shows good performance for CO_2 sorption of 0.64 gCO_2/gCaO at temperature 700°C. Kinetic model reveals that the sorption systems are controlled by both surface and diffusion through the layer.
2. The addition of anionic surfactants, SDS and Gemini surfactant, have influence on morphology of $CaCO_3$ of which rod-like structure is observed for SDS and needle-like is observed for Gemini surfactant.
3. Concentration of surfactant on CaO-based sorbent exhibits either positive or negative impact on CO_2 sorption capacity: CaO-SDS 20 mM and CaO-GS 2 mM can increase sorption capacity to 0.27 and 0.29 gCO_2/gCaO, respectively, at carbonation temperature of 600°C due to connected small particles of CaO-SDS 20 mM and high surface area (16.3 m^2/g) of CaO-GS 2 mM. CaO-SDS 40 mM and

CaO-GS 4 mM show negative effect because the interaction of surfactant on $CaCO_3$ promoted aggregation of small particles to large compact particle.

4. CaO-based sorbents, which synthesized by different techniques, distinguish morphologies structure and have an influence on CO_2 capture. The sorbent prepared by wet mixing and co-precipitation show large particles and rough surface, sol-gel exhibit uniformly small particles, and sol mixing provide small particles aggregation. The sol-gel sorbent offers good performance for CO_2 sorption of 0.65 $gCO_2/gCaO$. The sorption is observed to reduce to 0.41 $gCO_2/gCaO$ for 10 cycles of adsorption at 600°C under 15%CO_2 (balanced N_2).

7. Recommendation and future work

Our synthetic sorbents show good performance for CO_2 capture; however, a reduction of 35% sorption capacity in the 10th cycle is observed. A required stability for a long-term carbonation-decarbonation should be develoed.

In addition, further applications of CaO-based sorbent are also required. An interesting subject is the application of the sorbent for pre-combustion process i.e. sorption enhanced steam reforming process as not only CaO can enhance ability to produce hydrogen but also CO_2 emission can be reduced. However, for further implementation, the study on techno-economic analysis is recommended.

References

Akgsornpeak, A., Witoon, T., Mungcharoen, T., Limtrakul, J., 2014. Development of synthetic CaO sorbents via CTAB-assisted sol–gel method for CO_2 capture at high temperature. *Chemical Engineering Journal*, 237, 189–198.

Altay, E., Shahwan, T., Tanoğlu, M., 2007. Morphosynthesis of $CaCO_3$ at different reaction temperatures and the effects of PDDA, CTAB, and EDTA on the particle morphology and polymorph stability. *Powder Technology*, 178, 194-202.

Blamey, J., Anthony, E.J., Wang, J., Fennel, P.S., 2010. The calcium looping cycle for large-scale CO_2 capture. *Progress in Energy and Combustion Science*, 36, 260–279.

Broda, M., Kierzkowska, A. M., Müller C. R., 2012. Influence of the Calcination and Carbonation Conditions on the CO_2 Uptake of Synthetic Ca-Based CO_2 Sorbents. *Environ. Sci. Technol.*, 46, 10849–10856.

Craparo, Robert M. (2007). "Significance level". In Salkind, Neil J. Encyclopedia of Measurement and Statistics 3. Thousand Oaks, CA: SAGE Publications. pp. 889–891. ISBN 1-412-91611-9.

Cazorla-Amorb, D., Joly, J. P., Linares-Solano, A., Marcilla-Gomis, A., Salinas-Martinez de Lecea, C., 1991 CO_2-CaO Surface and Bulk Reactions: Thermodynamic and Kinetic Approach. *J . Phys. Chem.*, 95, 6611-6617.

Chanburanasiri, N., Ribeiro, Ana M., Rodrigues, Alirio E., Arpornwichanop, A., Laosiripojana, N., Praserthdam, P., Assabumrungrat, S., 2011. Hydrogen Production via Sorption Enhanced Steam Methane Reforming Process Using Ni/CaO Multifunctional Catalyst. *Ind. Eng. Chem. Res.*, 50, 13662-13671.

Chen, J., Xiang, L., 2009, Controllable synthesis of calcium carbonate polymorphs at different temperatures. *Powder Technology*, 189, 64–69.

Chen, Z., Li, C., Yang, Q., Nan, Z., 2010. Transformation of novel morphologies and polymorphs of $CaCO_3$ crystals induced by the anionic surfactant SDS. *Materials Chemistry and Physics.,* 123, 534–539.

Cho, Y.B., Seo, G., Chang, D.R., 2009. Transesterification of tributyrin with methanol over calcium oxide catalysts prepared from various precursors. *Fuel Processing Technology*, 90, 1252–1258.

Cobden, P.D., Elzinga, G.D., Booneveld, S., Dijkstra, J.W., Jansen, D., van den Brink, R.W., 2009. Sorption-enhanced steam-methane reforming: CaO-$CaCO_3$ capture technology. *Energy Procedia*, 1, 733-739.

Dou B., Song, Y., Liu, Y., Feng C., 2010. High temperature CO_2 capture using calcium oxide sorbent in a fixed-bed reactor. Journal of Hazardous Materials, 183, 759–765.

Florin, N. H., Harris, A. T., 2008. Preparation and Characterization of a Tailored Carbon Dioxide Sorbent for Enhanced Hydrogen Synthesis in Biomass Gasifiers. *Ind. Eng. Chem. Res.*, 47, 2191-2202.

Froment, G.F., 2001. Modeling of catalyst deactivation. *Applied Catalysis a-General*, 212, 117-128.

Harrison, D.P., 2009. Calcium enhanced hydrogen production with CO2 capture. *Energy Procedia*, 675-681.

Huang, J.H., Mao, Z.F., Luo, M.F., 2007. Effect of anionic surfactant on vaterite $CaCO_3$. *Materials Research Bulletin*, 42, 2184–2191.

Hufton, J.R., Mayorga, S., Sircar, S., 1999. Sorption-enhanced reaction process for hydrogen production. *Aiche Journal*, 45, 248-256.

Kim, J.N., Ko, C.H., Yi, K.B., 2013. Sorption enhanced hydrogen production using one-body CaO-$Ca_{12}Al_{14}O_{33}$-Ni composite as catalytic absorbent. *International Journal of Hydrogen Energy*, 38, 6072-6078.

Lee, K.B., Verdooren, A., Caram, H.S., Sircar, S., 2007. Chemisorption of carbon dioxide on potassium-carbonate-promoted hydrotalcite. *Journal of Colloid and Interface Science*, 308, 30-39.

Lee, K.B., Beaver, M.G., Caram, H.S., Sircar, S., 2008. Production of fuel-cell grade hydrogen by thermal swing sorption enhanced reaction concept. *International Journal of Hydrogen Energy*, 33, 781-790.

Li, L.Y., King, D. L., Nie, Z., Howard, C., 2009. Magnesia-Stabilized Calcium Oxide Absorbents with Improved Durability for High Temperature CO2 Capture. *Ind. Eng. Chem. Res.*, 48, 10604–10613.

Li, Z.S., Cai, N.S., Yang, J.B., 2006. Continuous production of hydrogen from sorption-enhanced steam methane reforming in two parallel fixed-bed reactors operated in a cyclic manner. *Industrial & Engineering Chemistry Research*, 45, 8788-8793.

Lu, H., Khan, A., Smirniotis, P. G., 2008. Relationship between Structural Properties and CO_2 Capture Performance of CaO-Based Sorbents Obtained from Different Organometallic Precursors. *Ind. Eng. Chem. Res*., 47, 6216–6220.

Reijers, H.T.J., Valster-Schiermeier, S.E.A., Cobden, P.D., van den Brink, R.W., 2006. Hydrotalcite as CO_2 sorbent for sorption-enhanced steam reforming of methane. *Ind. Eng. Chem. Res*., 45, 2522-2530.

Rout, K.R., Solsvik, J., Nayak, A.K., Jakobsen, H.A., 2011. A numerical study of multicomponent mass diffusion and convection in porous pellets for the sorption-enhanced steam methane reforming and desorption processes. *Chem. Eng. Sci.*, 66, 4111-4126.

Sircar, S., Lee, K.B., 2010. Sorption enhanced reaction concepts for hydrogen production. Material & Process, 1-211.

Steel, B.C.H., 2000. Materials for IT-SOFC stacks 35 years R&D: the inevitability of gradualness? Solid State Ionics 134, 3-20.

Wei, H., Shen, Q., Zhao, Y., Zhou, Y., Wang, D., Xu, D., 2005. On the crystallization of calcium carbonate modulated by anionic surfactants. *Journal of Crystal Growth*, 279, 439–446.

Xiu, G.H., Soares, J.L., Li, P., Rodrigues, A.E., 2002. Simulation of five-step one-bed sorption-enhanced reaction process. *Aiche Journal*, 48, 2817-2832.

Yu, J., Zhao, X., Cheng, B., Zhang, Q., 2005. Controlled synthesis of calcium carbonate in a mixed aqueous solution of PSMA and CTAB. *Journal of Solid State Chemistry*, 178, 861–867.

Zhou, Z., Qi, Y., Xie, M., Cheng, Z., Yuan W., 2012. Synthesis of CaO-based sorbents through incorporation of alumina/aluminate and their CO_2 capture performance. *Chemical Engineering Science*, 74, 172–180.

Appendix

Bibliography of project leader

Name	WORAPON KIATKITTIPONG
Position	Assistant Professor
Address (Office)	Department of Chemical Engineering, Faculty of Engineering and Industrial Technology, Silpakorn University, Nakhon Pathom 73000 Tel: (66)3-421-9364-6 ext. 25613; Fax: (66)3-421-9368
E-mail address	kiatkittipong_w @su.ac.th, worapon@hotmail.com

Educational Qualification

June 2005	D.Eng., Chemical Engineering, Chulalongkorn University
October 2001	M.Eng., Chemical Engineering, Chulalongkorn University
March 1999	B.Eng., Chemical Engineering, Kasetsart University

Academic Trip

April 2008 – Sep 2008	Guest Researcher in topic “Evaluating sorbent materials for metal removal”, Pacific Northwest National Laboratory (PNNL) under Battelle’s Office of Science & Engineering Education, Washington, USA
April 2003 –March 2004	Professor Goto’s laboratory, Department of Chemical Engineering, Nagoya University under AIEJ

Patent

หอกลั่นที่เกิดปฏิกิริยาสำหรับการผลิตไบโอดีเซลจากน้ำมันที่มีไตรกลีเซอไรด์และกรดไขมันอิสระเป็นองค์ประกอบ คณะผู้ประดิษฐ์ ศ.ดร.สุทธิชัย อัสสะบำรุงรัตน์ ณัจนันท์ บุญอนุวัฒน์ ผศ.ดร.วรพล เกียรติกิตติพงษ์ กนกวรรณ ง้าวสุวรรณ จุติพงศ์ ภูสุมาศ บำรุง สูงเนิน เลขที่คำขอ 1401004679

International publications

1) S. Phimsen, **W. Kiatkittipong***, H. Yamada, T. Tagawa, K. Kiatkittipong, N. Laosiripojana, S. Assabumrungrat, Oil Extracted from Spent Coffee Grounds for Bio-Hydrotreated Diesel Production, Energy Conversion and Management, (2016) DOI:10.1016/j.enconman.2016.08.085 (IF-2015 = 4.801)

2) T. Udomchoke, S. Wongsakulphasatch, **W. Kiatkittipong**, A. Arpornwichanop, W. Khaodee, J. Powell, J. Gong, S. Assabumrungrat, Performance evaluation of sorption enhanced chemical-looping reforming for hydrogen production from biomass with modification of catalyst and sorbent regeneration, Chemical Engineering Journal, 33, 338–347 (2016) (IF-2014 = 4.321)
3) C. Choomwattana, A. Chaianong, **W. Kiatkittipong**, P. Kongpannaa, A. T. Quitain, Suttichai Assabumrungrat, Process integration of dimethyl carbonate and ethylene glycol production from biomass and heat exchanger network design, Chemical Engineering and Processing, 107, 80-93 (2016) (IF-2014 = 2.071)
4) W. Khaodee, S. Wongsakulphasatch, **W. Kiatkittipong**, J. Powell, N. Laosiripojana**,** P. Bumroongsakulsawat, S. Assabumrungrat, Investigation of Biogas Decomposition Process for Fuel Cell Applications (PEMFC and SOFC): Thermodynamic Approach, Journal of Chemical Engineering of Japan, 49, 728-733 (2016) (IF-2014 = 0.644)
5) J. Phromprasit, J. Powell, S. Wongsakulphasatch, **W. Kiatkittipong**, P. Bumroongsakulsawat, S. Assabumrungrat, Activity and stability performance of multifunctional catalyst (Ni/CaO and Ni/$Ca_{12}Al_{14}O_{33}$-CaO) for bio-hydrogen production from sorption enhanced biogas steam reforming, International Journal of Hydrogen Energy, 41, 7318-7331 (2016) (IF-2014 = 3.313)
6) Natja-nan Boon-anuwat, **Worapon Kiatkittipong**, Farid Aiouache, Suttichai Assabumrungrat, “Process Design of Continuous Biodiesel Production by Reactive Distillation: Comparison between Homogeneous and Heterogeneous Catalysts” Chemical Engineering and Processing, 92, 33-44 (2015) (IF-2013 = 2.071)
7) Chayanit Choomwattana, Aksornchan Chaianong, **Worapon Kiatkittipong**, Pichayapan Kongpanna, Suttichai Assabumrungrat “Evaluation of Dimethyl Carbonate and Ethylene Glycol Production from Biomass”, Computer Aided Chemical Engineering, 37, 1295-1300 (2015) (SJR 2014 = 0.23)
8) Marisa Raita, **Worapon Kiatkittipong**, Navadol Laosiripojana, Verawat Champreda, Kinetic study on esterification of palmitic acid catalyzed by glycine-based cross linked protein coated microcrystalline lipase, Chemical Engineering Journal, 278, 19-23 (2015) (IF-2014 = 4.321)
9) T. Pairojpiriyakul, E. Croiset, K. Kiatkittipong, W. Kiatkittipong, A. Arpornwichanop, S. Assabumrungrat, “Catalytic reforming of glycerol in

supercritical water with nickel-based catalysts" International Journal of Hydrogen Energy, 39, 14739-14750 (2014) (IF-2014 = 3.313).

10) S. Wongsakulphasatch, W. Kiatkittipong, J. Saiswat, B. Oonkhanond, A. Striolo, S. Assabumrungrat, The adsorption aspect of Cu2+ and Zn2+ on MCM-41 and SDS-modified MCM-41, Inorganic Chemistry Communications, 46, 301-304 (2014) (IF-2013 = 2.062)
11) T. Pairojpiriyakul, W. Kiatkittipong, S. Assabumrungrat, E. Croiset, "Hydrogen production from supercritical water reforming of glycerol in an empty Inconel 625 reactor", International Journal of Hydrogen Energy 39 (1), 159-170 (2014) (IF-2013 = 2.930).
12) P. Piroonlerkgul, W. Kiatkittipong, S. Wongsakulphasatch, F. Aiouache, S. Assabumrungrat, "Evaluation of performance and operation viability of non-uniform potential solid oxide fuel cell fuelled by reformed methane" Journal of Power Sources 246 (2014) 719-728 (IF-2013 = 5.211)
13) W. Kiatkittipong*, S. Phimsen, K. Kiatkittipong, S. Wongsakulphasatch, N. Laosiripojana, S. Assabumrungrat, "Diesel-like hydrocarbon production from hydroprocessing of relevant refining palm oil", Fuel Processing Technology 116 (Dec 2013), 16–26 (2013) (IF-2013 = 3.019; SJR=1.479; SNIP=2.039) 14th in Jul-Sep 2013 of Top 25 Hottest Articles.
14) N. Lertlukkanasuk, S. Phiyanalinmat, W. Kiatkittipong, A. Arpornwichanop, F. Aiouache, S. Assabumrungrat, "Reactive Distillation for Synthesis of Glycerol Carbonate via Glycerolysis of Urea", Chemical Engineering and Processing: Process Intensification, 70 (Aug 2013), 103-109 (IF-2013 = 1.959)
15) S. Wongsakulphasatch, W. Kiatkittipong, S. Assabumrungrat, "Comparative study of fuel gas production for SOFC from steam and supercritical-water reforming of bioethanol" International Journal of Hydrogen Energy 38 (14), 5555-5562 (2013) (IF-2013 = 2.930).
16) T. Pairojpiriyakul, E. Croiset, W. Kiatkittipong, K. Kiatkittipong, A. Arpornwichanop, S. Assabumrungrat, "Hydrogen production from catalytic supercritical water reforming of glycerol with cobalt-based catalysts" International Journal of Hydrogen Energy, 38 (11), 4368-4379 (2013). 15th in April - June 2013 of Top 25 Hottest Articles
17) S. Assabumrungrat, J. Phromprasit, S. Boonkrue, W. Kiatkittipong, W. Wiyaratn, A. Soottitantawat, A. Arpornwichanop, N. Laosiripojana, J. Powell, "Energy Efficiency Evaluation for a ''Green'' Power Generation Process with Minimum Effort on Carbon Dioxide Capture and Storage" Chemical Engineering Communications 199 (12), 1642–1651 (2012) (IF-2012 = 1.052)

18) N. Triphob, S. Wongsakulphasatch, W. Kiatkittipong, T. Charinpanitkul, P. Praserthdam, S. Assabumrungrat, Integrated methane decomposition and solid oxide fuel cell for efficient electrical power generation and carbon capture" Chemical Engineering Research & Design 90 (12), 2223–2234 (2012) (IF-2012 = 1.927)
19) T. Pairojpiriyakul, W. Kiatkittipong, A. Soottitantawat, A. Arpornwichanop, N. Laosiripojana, W. Wiyaratn, E. Coiset and S. Assabumrungrat, "Thermodynamic analysis of hydrogen production from glycerol at energy self-sufficient conditions" Canadian Journal of Chemical Engineering 90 (5) 1112-1119 (2012) (IF-2012 = 1.003)
20) Worapon Kiatkittipong*, Suwimol Wongsakulphasatch, Nattapon Tintan, Navadol Laosiripojana, Piyasan Praserthdam and Suttichai Assabumrungrat, "Gasoline upgrading by self-etherification with ethanol on modified beta-zeolite" Fuel Processing Technology 92 (10) 1999-2004 (2011) (IF-2011 = 2.945)
21) Worapon Kiatkittipong*, Parinya Intaracharoen, Navadol Laosiripojana, Choowong Chaisuk, Piyasan Praserthdam, Suttichai Assabumrungrat, "Glycerol ethers synthesis from glycerol etherification with tert-butyl alcohol in reactive distillation" Computers and Chemical Engineering 35 (10) 2034-2043 (2011) (IF-2011 = 2.320) (23rd Jan-Mar 2011, 17th Apr-Jun 2011, 13rd Oct-Dec 2011, 7th in Jul-Sep 2011 and 13th in full year 2011 of Top 25 Hottest Articles)
22) W. Khaodee, S. Wongsakulphasatch, W. Kiatkittipong, A. Arpornwichanop, N. Laosiripojana, S. Assabumrungrat, "Selection of appropriate primary fuel for hydrogen production for different fuel cell types: Comparison between decomposition and steam reforming" International Journal of Hydrogen Energy 36 (13) 7696-7706 (2011) (IF-2011 = 4.054)
23) Navadol Laosiripojana, Worapon Kiatkittipong, Suttichai Assabumrungrat, "Partial oxidation of palm fatty acids over Ce-ZrO2: Roles of catalyst surface area, lattice oxygen capacity and mobility" AIChE Journal 57 (10) 2861-2869 (2011) (IF-2011 = 2.261)
24) Issara Choedkiatsakul, Kanokwan Ngaosuwan, Worapon Kiatkittipong, Navadol Laosiripojana and Suttichai Assabumrungrat, "Patent Review on "Biodiesel Production Process" Recent Patents on Chemical Engineering 4 (3), 265-279 (2011) (DOI: 10.2174/2211334711104030265)
25) I. Choedkiatsakul, S. Charojrochkul, W. Kiatkittipong, W. Wiyaratn, A. Soottitantawat, A. Arpornwichanop, N. Laosiripojana and S. Assabumrungrat, "Performance improvement of bioethanol-fuelled solid oxide fuel cell system

by using pervaporation" International Journal of Hydrogen Energy 36 (8) 5067-5075 (2011) (IF-2011 = 4.054)

26) G. Tanarungsun, H. Yamada, T. Tagawa, W. Kiatkittipong, P. Praserthdam and S. Assabumrungrat, "Partial oxidation of benzene catalyzed by vanadium chloride in novel reaction–extraction–regeneration system" Chemical Engineering and Processing: Process Intensification , 50 (1) 53-58 (2011) (IF-2011 = 1.924)
27) Vorachatra Sukwattanajaroon, Sumittra Charojrochkul, Worapon Kiatkittipong, Amornchai Arpornwichanop, and Suttichai Assabumrungrat, "Performance of Membrane-Assisted Solid Oxide Fuel Cell System Fuelled by Bioethanol" Engineering Journal, 15 (2), 53-66 (2011) (doi:10.4186/ej.2011.15.2.53) (SJR = 0.153, SNIP = 0.256)
28) Thirasak Pairojpiriyakul, Worapon Kiatkittipong, Amornchai Arpornwichanop, Apinan Soottitantawat, Wisitsree Wiyaratn, Navadol Laosiripojana, Eric Coiset and Suttichai Assabumrungrat, "Effect of mode of operation on hydrogen production from glycerol at thermal neutral conditions: Thermodynamic analysis", International Journal of Hydrogen Energy, 35 (19), 10257-10270 (2010) (IF-2010 = 4.035)
29) P. Piroonlerkgul, W. Kiatkittipong, A. Arpornwichanop, A. Soottitantawat, W. Wiyratn, N. Laosiripojana, A.A. Adesina and S. Assabumrungrat "Technical and economic study of integrated system of solid oxide fuel cell, palladium membrane reactor, and CO2 sorption enhancement unit" Chemical Engineering and Processing: Process Intensification, 49 (10), 1006-1016 (2010) (IF-2010 = 1.729)
30) N. Laosiripojana, W. Kiatkittipong, W. Sutthisripok, S. Assabumrungrat "Synthesis of methyl esters from relevant palm products in near-critical methanol with modified-zirconia catalysts" Bioresource Technology, 101 (21), 8416–8423 (2010) (IF-2010 = 4.365)
31) N. Laosiripojana, W. Kiatkittipong, S. Charojrochkul, S. Assabumrungrat "Effects of support and co-fed elements on steam reforming of palm fatty acid distillate (PFAD) over Rh-based catalysts" Applied Catalysis A: General, 383 (1-2), 50-57 (2010) (IF- 2010 = 3.383)
32) S. Assabumrungrat, P. Sonthisanga, W. Kiatkittipong, N. Laosiripojana, A. Arpornwichanop, A. Soottitantawat, W. Wiyaratn, P. Praserthdam "Thermodynamic analysis of calcium oxide assisted hydrogen production from biogas" Journal of Industrial and Engineering Chemistry, 16 (5), 785-789 (2010) (IF-2010 = 2.149).

33) Worapon Kiatkittipong*, Sirima Suwanmanee, Navadol Laosiripojana, Piyasan Praserthdam and Suttichai Assabumrungrat “Cleaner gasoline production by using glycerol as fuel extender” Fuel Processing Technology, 91 (5), 456-460 (2010) (IF-2010 = 2.781)
34) G. Tanarungsun, H. Yamada, T. Tagawa, W. Kiatkittipong, P. Praserthdam and S. Assabumrungrat “Reaction-extraction-regeneration system for highly selective oxidation of benzene to phenol” Chemical Engineering Communications, 197 (8), 1140-1151 (2010) (IF-2010 = 0.913)
35) I. Choedkiatsakul, K. Sintawarayan, T. Prawpipat, A. Soottitantawat, W. Wiyaratn, W. Kiatkittipong, A. Arpornwichanop, N. Laosiripojana, S. Charojrochkul and S. Assabumrungrat “Performance assessment of SOFC systems integrated with bio-ethanol production and purification processes” Engineering Journal, 14 (1), 1-14 (2010) (doi:10.4186/ej.2010.13.4.1)
36) P. Piroonlerkgul, W. Wiyaratn, A. Soottitantawat, W. Kiatkittipong, A. Arpornwichanop, N. Laosiripojana, S. Assabumrungrat “Operation viability and performance of solid oxide fuel cell fuelled by different feeds” Chemical Engineering Journal, 155 (1-2), 411-418 (2009) (IF- 2009 = 2.816)
37) S. Assabumrungrat, S. Charoenseri, N. Laosiripojana, W. Kiatkittipong, P. Praserthdam “Effect of oxygen addition on catalytic performance of Ni/SiO2.MgO toward carbon dioxide reforming of methane under periodic operation” International Journal of Hydrogen Energy, 34 (15), 6211-6220 (2009) (IF-2009 = 3.945)
38) O. Boonthumtirawuti, W. Kiatkittipong, A. Arpornwichanop, P. Praserthdam and S. Assabumrungrat “Kinetic of liquid phase synthesis of tert-amyl ethyl ether from tert-amyl alcohol and ethanol over Amberlyst 16” Journal of Industrial and Engineering Chemistry, 15 (4), 451-457 (2009) (IF-2009 = 1.752). (21st of Top, October to December 2009)
39) P. Piroonlerkgul, W. Kiatkittipong, A. Arpornwichanop, A. Soottitantawat, W. Wiyaratn, N. Laosiripojana, A.A. Adesina, S. Assabumrungrat “Integration of solid oxide fuel cell and palladium membrane reactor: Technical and economic analysis” International Journal of Hydrogen Energy, 34 (9), 3894-3907 (2009) (IF-2009 = 3.945)
40) Worapon Kiatkittipong*, Khamron Yoothongkham, Choowong Chaisuk, Piyasan Praserthdam, Shigeo Goto and Suttichai Assabumrungrat “Self-etherification process for cleaner fuel production” Catalysis Letters 128 (1-2), 154-163 (2009) (IF-2009 = 2.021)

41) Worapon Kiatkittipong, Porntip Wongsuchoto, Prasert Pavasant “Life cycle assessment of bagasse waste management options” Waste Management 29 (5), 1628-1633 (2009) (IF- 2009 = 2.433)
42) Vorapot Kanokkantapong, Worapon Kiatkittipong, Bunyarit Panyapinyopol, Porntip Wongsuchoto and Prasert Pavasant “Used lubricating oil management options based on life cycle thinking” Resources Conservation and Recycling, 53 (5), 294-299 (2009) (IF-2009 = 1.987)
43) S. Vivanpatarakij, N. Laosiripojana, W. Kiatkittipong, A. Arpornwichanopa, A. Soottitantawat, S. Assabumrungrat “Simulation of solid oxide fuel cell systems integrated with sequential CaO–CO2 capture unit” Chemical Engineering Journal, 147 (2-3), 336-341 (2009) (IF-2009 = 2.816)
44) A. Arpornwichanop, K. Koomsup, W. Kiatkittipong, P. Praserthdam, S. Assabumrungrat “Production of n-butyl acetate from dilute acetic acid and n-butanol using different reactive distillation systems: Economic analysis” Journal of the Taiwan Institute of Chemical Engineers, 40 (1), 21-28 (2009) (IF-2011 = 2.110) (3rd Top 25, July to September 2010)
45) N. Laosiripojana, W. Wiyaratn, W. Kiatkittipong, A. Arpornwichanop, A. Soottitantawat and S. Assabumrungrat “Reviews on Solid Oxide Fuel Cell Technology” Engineering Journal, 13 (1), 65-83 (2009) (doi:10.4186/ej.2009.13.1.65)
46) Worapon Kiatkittipong*, Piyaporn Thipsunet, Shigeo Goto, Choowong Chaisuk, Piyasan Praserthdam and Suttichai Assabumrungrat “Simultaneous enhancement of ethanol supplement in gasoline and its quality improvement” Fuel Processing Technology, 89 (12), 1365-1370 (2008) (IF-2008 = 2.066)
47) G. Tanarungsun, W. Kiatkittipong, P. Praserthdam, H. Yamada, T. Tagawa, and S. Assabumrungrat “Hydroxylation of benzene to phenol on Fe/TiO2 catalysts loaded with different types of second metal” Catalysis Communications, 9 (9), 1886-1890 (2008) (IF-2008 = 2.791) (13th of Top 25 Hottest Articles, April to June 2008)
48) G. Tanarungsun, W. Kiatkittipong, P. Praserthdam, H. Yamada, T. Tagawa and S. Assabumrungrat “Ternary metal oxide catalysts for selective oxidation of benzene to phenol” Journal of Industrial and Engineering Chemistry, 14 (5) 596-601 (2008) (IF- 2008 = 1.235)
49) Worapon Kiatkittipong, Porntip Wongsuchoto, Khanidtha Meewasana and Prasert Pavasant “When to buy new electrical/electronic products?” Journal of Cleaner Production, 16 (13), 1339-1345 (2008) (IF-2008 = 1.362)

50) G. Tanarungsun, W. Kiatkittipong, S. Assabumrungrat, H. Yamada, T. Tagawa and P. Praserthdam “Multi transition metal catalysts supported on TiO2 for hydroxylation of benzene to phenol with hydrogen peroxide” Journal of Industrial and Engineering Chemistry, 13 (5), 870-877 (2007) (IF-2007 = 1.570).
51) G. Tanarungsun, W. Kiatkittipong, S. Assabumrungrat, H. Yamada, T. Tagawa and P. Praserthdam “Liquid phase hydroxylation of benzene to phenol with hydrogen peroxide catalyzed by Fe (III)/TiO2 catalysts at room temperature” Journal of Industrial and Engineering Chemistry, 13 (3), 444-451 (2007) (IF-2007 = 1.570).
52) G. Tanarungsun, W. Kiatkittipong, S. Assabumrungrat, H. Yamada, T. Tagawa and P. Praserthdam “Fe (III), Cu (II), V (V)/TiO2 for hydroxylation of benzene to phenol with hydrogen peroxide at room temperature” Journal of Chemical Engineering of Japan, 40 (5), 415-421 (2007) (IF-2007 = 0.594).
53) Worapon Kiatkittipong, Tomohiko Tagawa, Shigeo Goto, Suttichai Assabumrungrat, Kampol Silpasup and Piyasan Praserthdam, “Comparative Study of Oxidative Coupling of Methane Modeling in Various Types of Reactor” Chemical Engineering Journal, 115 (1-2), 63-71 (2005) (4th of TOP 25 Hottest Articles, October to December 2005) (IF-2005 = 2.034).
54) Worapon Kiatkittipong, Shigeo Goto, Tomohiko Tagawa, Suttichai Assabumrungrat and Piyasan Praserthdam “Simulation of Oxidative Coupling of Methane in Solid Oxide Fuel Cell Type Reactor for C 2Hydrocarbons and Electricity Co-Generation” Journal of Chemical Engineering of Japan, 38 (10), 841-848 (2005) (IF-2005 = 51.09).
55) Worapon Kiatkittipong, Tomohiko Tagawa, Shigeo Goto, Suttichai Assabumrungrat and Piyasan Praserthdam “Oxygen transport through LSM/YSZ/LaAlO system for the use of fuel cell type reactor” Chemical Engineering Journal, 106 (1), 35-42 (2005) (IF-2005 = 2.034).
56) Worapon Kiatkittipong, Tomohiko Tagawa, Shigeo Goto, Suttichai Assabumrungrat and Piyasan Praserthdam “Oxidative Coupling of Methane in LSM/YSZ/LaAlO SOFC Reactor” Journal of Chemical Engineering of Japan 37 (12), 1461-1470 (2004) (IF-.(515.0 = 2004
57) Worapon Kiatkittipong, Tomohiko Tagawa, Shigeo Goto, Suttichai Assabumrungrat and Piyasan Praserthdam “TPD study in LSM/YSZ/LaAlO system for the use of fuel cell type reactor” Solid State Ionics, 166 (1-2), -127 136(2004) (IF- 2004 = .1862).
58) Suttichai Assabumrungrat, Worapon Kiatkittipong, Piyasan Praserthdam and Shigeo Goto “Simulation of pervaporation membrane reactors for liquid phase

synthesis of ethyl tert-butyl ether from tert-butyl alcohol and ethanol" Catalysis Today, 80-79, 2) (2003) 257-49IF-.(627.2 = 2003

59) Worapon Kiatkittipong, Suttichai Assabumrungrat, Piyasan Praserthdam and Shigeo Goto, "A pervaporation membrane reactor for liquid phase synthesis of ethyl tert-butyl ether from tert-butyl alcohol and ethanol", Journal of Chemical Engineering of Japan 35 (6), 547-556 (2002) (IF-2002 = 0.459).
60) Assabumrungrat S, Kiatkittipong W, Srivitoon N, Praserthdam P, Goto S, "Kinetics of liquid phase synthesis of ethyl tert-butyl ether from tert-butyl alcohol and ethanol catalyzed by β-zeolite supported on monolith", International Journal of Chemical Kinetics, 299-292 (5) :34, May) 2002IF- 2002 (086.1 =
61) Worapon Kiatkittipong, Suttichai Assabumrungrat and Piyasan Praserthdam, "Synthesis of ethyl tert-butyl ether from tert-butyl alcohol and ethanol catalyzed by β-zeolite in pervaporative membrane reactors", Journal of The Institution of Engineers Singapore (Chemical Engineering) vol. 42 (2) 6-10, 2002.

Book Chapter

1) Vorachatra Sukwattanajaroon, Suttichai Assabumrungrat, Sumittra Charojrochkul, Navadol Laosiripojana and Worapon Kiatkittipong "Bioethanol-Fuelled Solid Oxide Fuel Cell System for Electrical Power Generation" Renewable Energy - Trends and Applications, ISBN 978-953-307-939-4, InTech 2011; 9: 191-212 (Published: November 9, 2011).